

**PREPARATION AND CHARACTERIZATION OF  
CARTILAGE MIMICKED STRUCTURES**

by

**MEFTUNE ÖZGEN ÖZTÜRK**

B.S., Chemical Engineering, Hacettepe University, 2011

Submitted to the Institute of Biomedical Engineering  
in partial fulfillment of the requirements  
for the degree of  
Master of Science  
in  
Biomedical Engineering

Boğaziçi University

2014

**PREPARATION AND CHARACTERIZATION OF  
CARTILAGE MIMICKED STRUCTURES**

**APPROVED BY:**

Assist. Prof. Dr. Bora Garipcan .....

(Thesis Advisor)

Assoc. Prof. Dr. Burak Güçlü .....

Assoc. Prof. Dr. Kadriye Tuzlakoglu .....

**DATE OF APPROVAL:** 30 January 2014

## ACKNOWLEDGMENTS

I would like to thank my advisor, Assist. Prof. Dr. Bora Garipcan, for his guidance and advices. I thank Assoc. Dr. Deniz Hür, Assoc. Dr. Lokman Uzun and Assist Dr. Çağlar Elbüken for their help.

I thank Assoc. Prof. Dr. Güçlü and Assoc. Prof. Dr. Kadriye Tuzlakoglu for their precious comments and contribution.

I thank TÜBİTAK for their support on our project "Synthesis, Characterization and Applications of Novel Amido Amino Acid Self-Assembled Molecules" (Project number: 112T564).

I specially thank my friends; Nehar Çelikkın, Öznur Demir, Murat Can Mutlu, Selin Yalvarmış, Umut Öncel and all my laboratory colleagues for their support, understanding and motivation.

I owe my deepest gratitude to my sister, my aunt, my mum and my dad for their support, patience and encouragement.

## ABSTRACT

### PREPARATION AND CHARACTERIZATION OF CARTILAGE MIMICKED STRUCTURES

In this thesis, micro-environment of cartilage tissue was mimicked by adjusting the surface topography, stiffness and chemistry of polydimethylsiloxane (PDMS) which is a biocompatible synthetic elastomeric polymer. PDMS substrates were synthesized with different stiffness between  $2.13 \pm 0.150$  MPa and  $0.56 \pm 0.06$  MPa which were in the range of healthy human articular cartilage's stiffness (0.45-0.80 MPa) and measured by nanoindentation. A template mimicking the collagen type II bundle alignment, geometry and size of healthy human cartilage tissue were prepared (A= 100, 150, 200  $\mu\text{m}$ ; B= 30, 40, 50  $\mu\text{m}$ ; C= 30, 40, 50  $\mu\text{m}$ ) by photolithography. PDMS substrates with desired patterns were prepared by soft lithography. In order to mimic the chemistry of the cartilage tissue micro-environment, PDMS substrates were modified with amino acid conjugated self-assembled molecules (Histidine, Leucine and Tryptophan) and also with type II collagen. Stiffness of PDMS substrates were analyzed with nanoindentation measurements and chemical modifications of substrates were confirmed by using X-ray Photoelectron Spectroscopy and contact angle measurements. According to the characterization results, prepared substrates with cartilage like stiffness, chemistry and topography are possible cell substrates for cartilage tissue engineering.

**Keywords:** Cartilage-mimicked structures, Polydimethylsiloxane (PDMS), Stiffness, Amino acids, Self-assembled Molecules (SAMs)

## ÖZET

### KIKIRDAK TAKLİDİ YAPILARIN SENTEZİ VE KARAKTERİZASYONU

Bu tez çalışmasında, biyouyumlu, sentetik ve elastomerik bir polimer olan PDMS'in yüzey topografisi, sertliği ve kimyası, kıkırdağın mikro-çevresine ayarlanarak, kıkırdak dokusu taklit edilmiştir. Nanoiz yöntemiyle sertlikleri belirlenen PDMS substratları,  $2.13 \pm 0.150$  MPa ve  $0.56 \pm 0.06$  MPa arası sertliklerde sentezlenmiştir. Bu değerlerin sağlıklı insan kıkırdağının sertliğine uyumu (0.45-0.80 MPa) görülmüştür. Sağlıklı insan kıkırdağındaki tip II kolajen demetlerinin yönelme, geometri ve uzunluklarını taklit eden kalıplar tasarlanmış (A= 100, 150, 200  $\mu\text{m}$ ; B= 30, 40, 50  $\mu\text{m}$ ; C= 30, 40, 50  $\mu\text{m}$ ) ve fotolitografi yöntemiyle hazırlanmıştır. PDMS substratların desenlemesi, tasarlanan kalıp kullanılarak yumuşak litografi ile elde edilmiştir. Kıkırdak dokusunun mikro-çevresinin kimyasını taklit etmek için, PDMS substratlar amino asit konjüge kendiliğinden yönelen moleküller (histidin, lözin ve triptofan) ile tip II kolajen kullanılarak modifiye edilmişlerdir. PDMS substratların sertlikleri nanoiz yöntemi ile ölçülmüş, kimyasal modifikasyonlarının başarısı da X ışını fotoelektron spektroskopisi ve temas açısı ölçümleri kullanılarak kanıtlanmıştır. Karakterizasyon sonuçlarına göre, kıkırdak benzeri sertlik, yüzey kimyası ve yüzey topografisi ile hazırlanan PDMS substratların, kıkırdak doku mühendisliği için bir iyi hücre substratı adayı olduğu görülmüştür.

**Anahtar Sözcükler:** , Kıkırdak benzeri yapılar, Polidimetilsiloksan (PDMS), Sertlik, Amino asitler, Kendiliğinden düzenlenen moleküller (KDM).

## TABLE OF CONTENTS

ACKNOWLEDGMENTS . . . . .	iii
ABSTRACT . . . . .	iv
ÖZET . . . . .	v
LIST OF FIGURES . . . . .	viii
LIST OF TABLES . . . . .	x
LIST OF SYMBOLS . . . . .	xii
LIST OF ABBREVIATIONS . . . . .	xiii
1. INTRODUCTION . . . . .	1
1.1 Motivation . . . . .	1
1.2 Objectives . . . . .	3
1.3 Outline . . . . .	3
2. BACKGROUND . . . . .	4
2.1 Articular Cartilage: Structure and Function . . . . .	4
2.2 Cartilage Defects and Regeneration . . . . .	7
2.3 Cartilage Tissue Engineering and Cell Based Therapies . . . . .	8
2.4 Effects of cell substrate properties on stem cell differentiation . . . . .	10
2.5 Polymeric Materials for Cartilage Tissue Engineering and Polydimethyl- siloxane . . . . .	12
3. MATERIALS AND METHODS . . . . .	14
3.1 Surface Preparation . . . . .	14
3.1.1 Preparation of Plain PDMS Substrates . . . . .	14
3.1.2 Preparation of Patterned PDMS Substrates . . . . .	14
3.1.3 Chemical Modification of PDMS Substrates . . . . .	16
3.1.3.1 Modification of PDMS Substrates with APTES . . . . .	16
3.1.3.2 Synthesis of Amino Acid Conjugated Self Assembled Molecules . . . . .	17
3.1.3.3 Modification of PDMS Substrates with SAMs . . . . .	18
3.1.3.4 Modification of PDMS Substrates with Type II Collagen	19
3.2 Surface Characterization . . . . .	19

3.2.1	Characterization of Mechanical Properties of PDMS Substrates	19
3.2.2	Characterization of Patterned PDMS Substrates . . . . .	21
3.2.3	X-ray Photoelectron Spectroscopy (XPS) . . . . .	21
3.2.4	Contact Angle Measurements . . . . .	21
4.	RESULTS . . . . .	22
4.1	Nanoindentation Measurements of PDMS Substrates . . . . .	22
4.2	Optical Microscopy . . . . .	22
4.3	Characterization of Amino Acid Conjugated Self Assembled Molecules .	23
4.4	Contact Angle Measurements . . . . .	26
4.4.1	Contact Angle Measurements of Bare PDMS Substrates with Different Prepolymer/Cross linker Ratios . . . . .	26
4.4.2	Contact Angle Measurements of Bare and APTES (1% v/v) Modified PDMS Substrates . . . . .	27
4.4.3	Contact Angle Measurements of His-SAM Modified PDMS Sub- strates . . . . .	27
4.4.4	Contact Angle Measurements for His-SAM, Leu-SAM, Trp-SAM and Collagen type II Modified PDMS Substrates . . . . .	29
4.5	X-ray Photoelectron Spectroscopy (XPS) Analysis . . . . .	30
4.5.1	XPS Analysis of Bare PDMS . . . . .	30
4.5.2	XPS analysis of APTES modified PDMS substrates . . . . .	31
4.5.3	XPS Analysis of His-SAM Modified PDMS Substrates . . . . .	33
4.5.4	XPS analysis of Leu-SAM modified PDMS substrates . . . . .	35
4.5.5	XPS analysis of Trp-SAM modified PDMS substrates . . . . .	37
4.5.6	XPS analysis of Type II Collagen Modified PDMS Substrates .	39
5.	DISCUSSION . . . . .	41
5.1	Stiffness of PDMS substrates . . . . .	41
5.2	Surface Topography of PDMS Substrates . . . . .	42
5.3	Chemical modifications of PDMS substrates . . . . .	43
5.4	Future Work . . . . .	47
	REFERENCES . . . . .	48

## LIST OF FIGURES

Figure 2.1	A cross-sectional diagram through a synovial joint	5
Figure 2.2	Alignment of collagen type II bundles a) Transmission Electron Microscopy (TEM) image of collagen type II bundles; b) Collagen type II, IX and XI alignment	6
Figure 2.3	Collagen orientation and chondrocyte appearance in different zones of cartilage tissue	7
Figure 2.4	Differences between bone and cartilage healing processes	8
Figure 2.5	Examples of topographical effects on cellular behaviour	10
Figure 2.6	Sensitivity of cells to surface topography through focal adhesions	11
Figure 3.1	Geometry and size of type II collagen bundles-like template	15
Figure 3.2	APTES modified PDMS	17
Figure 3.3	General synthesis procedure for the amino acid conjugated self assembled molecules	18
Figure 3.4	Amino acid conjugated SAMs on PDMS substrate a) His-SAM, b) Leu-SAM, c) Trp-SAM	18
Figure 3.5	a) CellHesion <sup>®</sup> 200, b) Pyramidal tip of a CONT cantilever.	20
Figure 4.1	Young's moduli data of PDMS, w/w; prepolymer-crosslinker ratio. Measured with CellHesion <sup>®</sup> 200 by using Hertz model, in air, at 25°C, p<0.0001	22
Figure 4.2	Surface patterning on PDMS substrate	23
Figure 4.3	1H NMR spectrum of Leu-SAM	24
Figure 4.4	1H NMR spectrum of Leu-SAM	25
Figure 4.5	1H NMR spectrum of Trp-SAM	25
Figure 4.6	Captured photos of the water drops on the PDMS surfaces with different prepolymer/ crosslinker ratios	26
Figure 4.7	Captured photos of the water drops on a) bare and b) APTES modified PDMS.	27
Figure 4.8	Captured photos of the water drops on His-SAM modified PDMS substrates a) 1mM, b) 2 mM, c) 5 mM, d) 10 mM, e) 20 Mm	28



Figure 4.9	Captured photos of the water drops of His-SAM (10mM) modified PDMS substrates; A) 1h, b) 2h, C) 4h, D) 24h	29
Figure 4.10	Contact Angle Measurements for His-SAM, Leu-SAM, Trp-SAM and Collagen type II Modified PDMS Substrates	30
Figure 4.11	XPS spectra of bare PDMS with survey spectrum, Si2p, O1s, and C1s regions	31
Figure 4.12	XPS survey spectrum of APTES modified PDMS substrate	32
Figure 4.13	XPS spectra of Aptes modified PDMS with Si2p, C1s, O1s and N1s	32
Figure 4.14	XPS survey spectrum of His-SAM (10mM) modified PDMS substrate	34
Figure 4.15	XPS spectra of His-SAM (10mM) modified PDMS with Si2p, C1s, O1s and N1s regions	35
Figure 4.16	XPS survey spectrum of Leu-SAM (10mM, 2h) modified PDMS substrate	36
Figure 4.17	XPS spectra of Leu-SAM (10mM,2h) modified PDMS with Si2p, C1s, O1s and N1s regions	36
Figure 4.18	XPS survey spectrum of Trp-SAM (10mM, 2h) modified PDMS substrate	37
Figure 4.19	XPS spectra of Trp-SAM (10mM) modified PDMS with Si2p, C1s, O1s and N1s regions	38
Figure 4.20	XPS survey spectrum of Type II collagen modified PDMS substrate	39
Figure 4.21	XPS spectra of Type II collagen modified PDMS with Si2p, C1s, O1s and N1s regions	40

## LIST OF TABLES

Table 2.1	Natural and synthetic polymers used in cartilage tissue engineering	13
Table 3.1	Pattern dimensions of Collagen Type II bundles-like template	15
Table 4.1	Contact angle measurements of Bare PDMS with different pre polymer-crosslinker ratios.	26
Table 4.2	Contact angle measurements of Bare and APTES modified PDMS substrates	27
Table 4.3	Contact angle measurements of His-SAM modified PDMS substrates with different concentration and dipping time	28
Table 4.4	Contact Angle Measurements of His-SAM modified PDMS substrates with different dipping time (1-24h), His-SAM Concentration: 10 mM; in air, at 25°C	29
Table 4.5	Contact Angle Measurements of His-SAM modified PDMS substrates with different dipping time (1-24h), His-SAM Concentration: 10 mM; in air, at 25°C	30
Table 4.6	Theoretical and measured atomic percentages of C, O and Si atoms found in PDMS	31
Table 4.7	Theoretical and measured atomic percentages of C, O, N and Si atoms found in APTES modified PDMS substrates	33
Table 4.8	Theoretical and measured atomic percentages of C, O, N and Si atoms found in modified PDMS substrate different His-SAM concentration	33
Table 4.9	Theoretical and measured atomic percentages of C, O, N and Si atoms found in modified PDMS substrate with different dipping time of His-SAM	34
Table 4.10	Theoretical and measured atomic percentages of C, O, N and Si atoms found in Leu-SAM modified PDMS	37
Table 4.11	Theoretical and measured atomic percentages of C, O, N and Si atoms found in Trp-SAM modified PDMS	38

Table 4.12	Theoretical and measured atomic percentages of C, O, N and Si atoms found in Type II collagen modified PDMS	40
------------	---	----

## LIST OF SYMBOLS

E	Young's Modulus
F	Force
L	Length
A	Area

## LIST OF ABBREVIATIONS

PDMS	Polydimethylsiloxane
SAM	Self assembled molecule
His-SAM	Histidine conjugated self assembled molecule
Leu-SAM	Leucine conjugated self assembled molecule
Trp-SAM	Tryptophan conjugated self assembled molecule
ECM	Extracellular matrix
GAG	Glycosaminoglycan
TEM	Transmission electron microscopy
MSC	Mesenchymal stem cell
PLCL	Poly (L-lactide-co-3-caprolactone)
PGA	Polyglycolic acid (PGA)
PLA	Polylactic acid
PLGA	Polylactic-co-glycolic acid
IPA	Isopropanol
RT	Room temperature
DI	Deionized water
UV	Ultraviolet
APTES	(3-Aminopropyl)triethoxysilane
THF	Tetrahydrofuran
HCl	Hydrochloric acid
DMSO	Dimethyl sulfoxide
XPS	X-ray photoelectron microscopy
NMR	Nuclear magnetic resonance
Cbz-AA-Bt	Carbobenzyloxy Amino acid Benzotriazole

# 1. INTRODUCTION

## 1.1 Motivation

Cartilage is a flexible connective tissue which bears the ends of bones and helps us to move. The structure and function of this tissue is unique and cartilage can be easily damaged from daily activities [1]. Many people around the world are suffering from osteoarthritis which is a degenerative condition caused from the break down of cartilage during daily physical activities or aging. Due to lack of blood supply, cartilage's self-regeneration capacity is relatively very low and if left untreated, causes pain, swelling and ultimately loss of joint function [2]. However, current medication for cartilage defects is only for pain relief. They cannot initiate cartilage healing. Since, surgical replacement looks like the only treatment preferably by using autographs which have to be donated and hard to obtain. Also there are many unsuccessful replacement experiments which increases the interest of cartilage tissue engineering to repair cartilage defects [3, 4, 5, 6].

Cartilage tissue engineering has been a great hope for a long term treatment of the defected cartilage tissue. In cartilage tissue engineering, chondrocytes are grown and populated by using appropriate cell sources, appropriate biomaterials and appropriate culture conditions [7]. Major drawback of these studies is losing the function, morphology and shape of chondrocytes, called dedifferentiation. It causes the cells lose their chondrogenic behaviour to regenerate cartilage and efficiency of the treatment decreases. Used cell type, and contact of cells with flat, rigid surfaces are main reasons of cell dedifferentiation [8]. Thus properties of cell substrates are crucial for cartilage tissue engineering.

Recent studies show that, living cells can realize stiffness, topography, chemical and biochemical composition of their surroundings response according to this input [9]. Among these studies Liu (2013) reported the chemical functionality of cell substrate can affect the behaviour of human adipose derived stem cells (hASCs), after producing plasma polymerized films, rich in amine (-NH<sub>2</sub>), carboxyl (-COOH) and methyl

(-CH<sub>3</sub>) on hydroxyapatite substrates and investigated osteogenic differentiation [10]. Results of this study showed that, osteogenic differentiation was promoted in -NH<sub>2</sub> modified surfaces. Greater amount of proteins were absorbed by -COOH modified surfaces and -CH<sub>3</sub> modification was not a successful modification for osteogenic differentiation and protein absorption of cells [10].

Biomechanical forces, such as surface stiffness, are important to regulate extracellular matrix to change in shape and size and thus effect stem cell differentiation. In 2006 Engler et al. showed the effect substrate stiffness on stem cell differentiation. They indicated that collagen I-coated firm gels with muscle mimicked elasticity caused stem cells to upregulate myogenic markers [1].

In an another study, effects of surface topography on stem cell differentiation was investigated. Alterations of geometry and size of the substrate influence cell adhesive molecules and eventually change the number and distribution of focal adhesions. These changes in focal adhesions may enhance cell growth, adhesion, motility and stem cell differentiation. For example, random features lead to osteogenic differentiation of Mesenchymal stem cells and anisotropic features induced axon outgrowth guidance in neurons [11].

With the inspiration of these studies, to enhance a better cellular activity, to induce chondrogenic stem cell differentiation and to inhibit dedifferentiation of chondrocytes, preparing substrates with cartilage-like chemical, mechanical and topographical properties are holding a great promise [11].

## 1.2 Objectives

In this thesis, PDMS was used as a cell substrate as it is non-toxic, biocompatible and has tunable mechanical properties. Stiffness of PDMS was adjusted to human cartilage tissue's stiffness. Alignment, geometry and size of collagen type II bundles were mimicked on PDMS substrate's surface and substrate surface was modified with amino acid conjugated self assembled molecules to prepare cartilage extracellular matrix-like environment. The main objectives of this study are:

- The production of polydimethylsiloxane (PDMS) cell substrates mimicking cartilage tissue's elasticity,
- Adjusting the surface topography of substrates to the type II collagen fibers, which are found predominantly (approximately 90% of total collagen) [2] in cartilage tissue,
- Modifying the surface with amino acid conjugated self assembled molecules and to characterize these substrates,
- Modifying the surface with type II collagen.

## 1.3 Outline

The thesis is presented as follows; In chapter 2, background information about cartilage tissue, cartilage tissue engineering, appropriate cell substrates and required modifications of cell substrates is explained. In chapter 3, the experimental procedures are explained. In chapter 4, the results are presented In chapter 5, the discussion of the results are given.



## 2. BACKGROUND

Cartilage is a living, firm and elastic connective tissue which is found in many areas of the body, including the joints, ribs, nose, ear, trachea and intervertebral discs. It performs different functions, as structural support, shape maintenance or shock absorber. Cartilage tissue is found in various forms in the body. It is classified depending on its composition as articular (also known as hyaline) cartilage, fibrocartilage, or elastic cartilage. Articular cartilage, which is white-blue in colour, smooth and glistening, is the most abundant type among the cartilage types mentioned above [1, 12].

### 2.1 Articular Cartilage: Structure and Function

The articulating bond ends in diarthrodial joints are covered by the articular cartilage which distribute the loads by minimizing the friction and shock absorption. Articular cartilage is a soft but strong tissue. Its characteristic stiffness helps to reduce contact stresses at joints [1]. Young's modulus of cartilage is in the range of 5-25 MPa depending on the depth and type of the joint. The compressive aggregate modulus fall within the range of 0.08 to 2 MPa, with an average range of 0.45 to 0.80 MPa [13]. For comparison, the Young's modulus in the midshaft of a long bone varies from about 17 GPa in the longitudinal direction to about 12 GPa in the transverse direction [14]. These data show that cartilage has a much lower stiffness (modulus) than bone[15].

Articular cartilage is composed of relatively low numbers of highly specialized cells, called chondrocytes, and a multicomponent extracellular matrix, which is secreted by chondrocytes and primarily composed of water, proteoglycans, collagens, elastin, glycoproteins and interstitial fluid. Chondrocytes are located in the lacunae and they receive their nutrition from synovial fluid via diffusion [12]. Chondrocytes produce the extracellular matrix which has a water content of approximately 70 to 85%. The remainder of the tissue is mainly proteoglycans and collagen [1]. This composition provides cartilage viscoelastic properties. Proteoglycans, which approximately 30% of

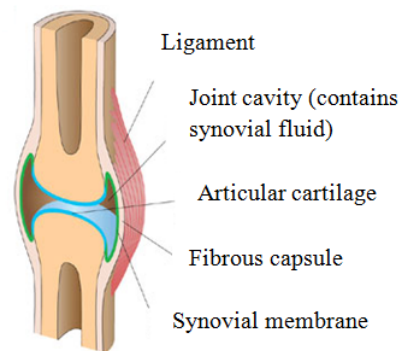


**Figure 2.1** A cross-sectional diagram through a synovial joint [16].

the dry weight of articular cartilage form a bottlebrush-like structure consisting of a core protein (aggrecan, biglycan, decorin in the extracellular matrix; syndecan, CD44 and fibroglycan as cell surface receptors; serglycan in intracellular tissues) which is attached to glycosaminoglycans. These GAG side chains, keratan and chondroitin sulphate help water retention of the tissue. Proteoglycans are bind to a hyaluronic acid backbone to form a macromolecule [1, 12].

Collagen is a fibrous protein that makes two-thirds of the dry mass of articular cartilage [1]. Type II is the predominant collagen in articular cartilage, but collagen III, VI, IX, X, XI, XII and XIV are all found in the extracellular matrix [17]. Among all the collagens found in the cartilage tissue, 90-95% of the collagen present is in the form of collagen type II bundles [13]. It forms a meshwork that encloses massive proteoglycan aggregates. This conjunction (the alignment of collagen type II bundles and the rigidity of proteoglycans) provide compressive load strength to the cartilage tissue [1].

Proteoglycan, collagen and water content vary through the depth of the cartilage tissue. There are four different regions between the articular surface and subchondral bone classified by these structural differences: the superficial tangential zone, the intermediate or middle zone, the deep or radiate zone and the calcified zone. The orientation of collagen bundles are different in these zones. In calcified and deep zones they are radially oriented, while from the upper deep zone into the middle zone they become less distinct. The finest fibers are found in the superficial zone and that's why sometimes this zone is referred as the gliding zone. Collagen in superficial zone is randomly oriented and it is parallel to the joint surface. This orientation helps the

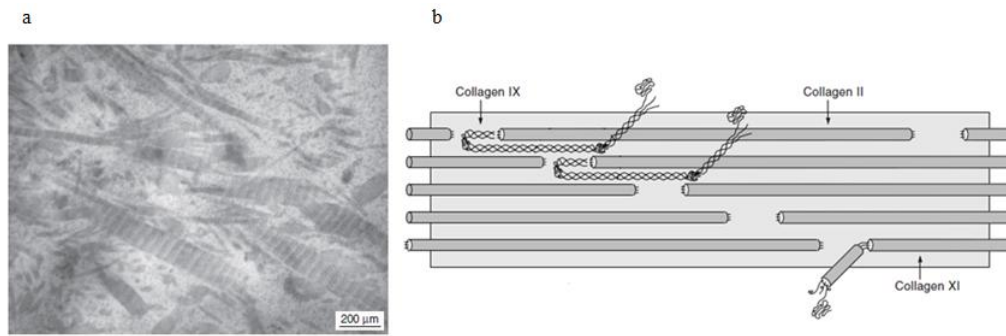


**Figure 2.2** Alignment of collagen type II bundles a) Transmission Electron Microscopy (TEM) image of collagen type II bundles [13]; b) Collagen type II, IX and XI alignment [17].

tissue to resist compressive forces. Highest water content and few proteoglycan aggregates are found in superficial zone. Also in deeper regions of cartilage, proteoglycan concentration is very high and near the articular surface it is lower [1, 18].

Articular cartilage helps to maintain body's shape, provides structural support and absorbs shock during physical exercise. This mechanical behaviour of cartilage arises from its special constituents; collagen and proteoglycans. Proteoglycans are negatively charged in aqueous environment and the repulsive forces of this negative charges cause aggregated proteoglycan molecules to expand. As proteoglycans are located in the collagen framework, their spreading volume is limited. However the enlargement of these aggregated molecules against collagen is the basic principle of cartilage's mechanical response. In the compression of the tissue, negatively charged sites on aggregan aggregate, repulsive force increases and so does the compressive stiffness of cartilage [1, 12].

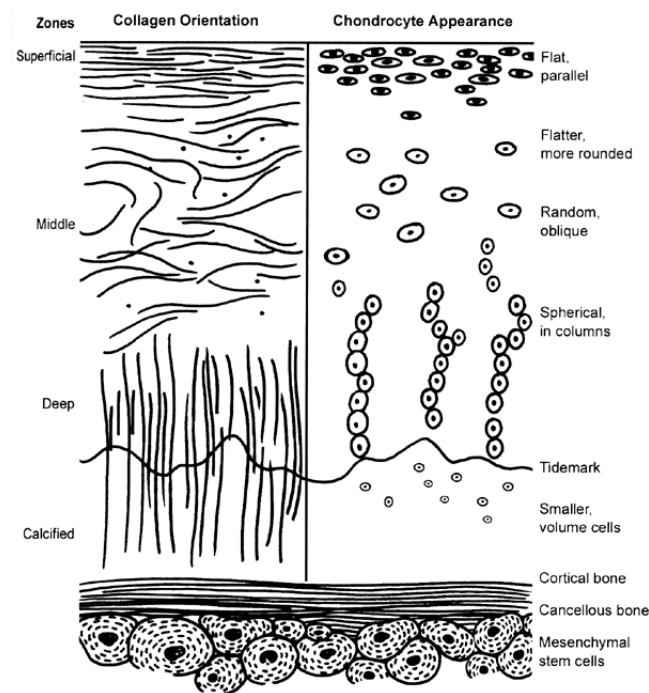


**Figure 2.3** Collagen orientation and chondrocyte appearance in different zones of cartilage tissue [18].

## 2.2 Cartilage Defects and Regeneration

Due to trauma or osteochondral pathology, such as osteonecrosis and osteochondritis dissecans, cartilage tissue may lose its joint function and this may lead to disability. Many people around the world are suffering from osteoarthritis, which is a degenerative condition caused by the breakdown of cartilage during daily physical activities or aging. In adults, cartilage tissue healing is very poor and if left untreated, causes pain, swelling, and ultimately loss of joint function [2, 3].

Most of the chondrocytes are found near the osteochondral junction and are captured with extracellular matrix constituents, so they have a limited migration ability. Furthermore, cartilage tissue consists of a relatively low number of cells because of its avascular nature, which causes a hypoxic environment and a lack of lymphatic vessels. Thus, after the injury, the normal inflammation process does not occur, and consequently, the tissue cannot heal [2]. Another drawback of having a low number of chondrocytes is the poor regeneration of the extracellular matrix. As mentioned before, the cartilage extracellular matrix components (including collagen II, which forms the network) are

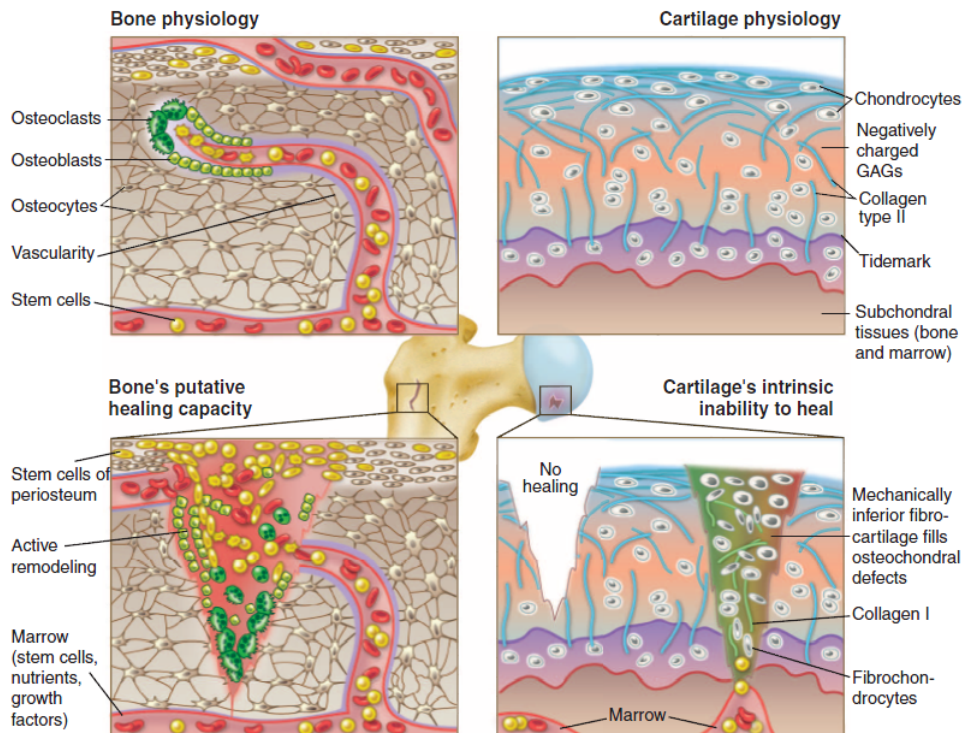


**Figure 2.4** Differences between bone and cartilage healing processes [19].

synthesized by chondrocytes. The low density of these cells and lack of nutrient supply cause cartilage tissue a very poor self-healing capacity [19, 20].

Several researches showed that there is no existing medication to initiate cartilage healing. The recommended therapy is surgical replacement for cartilage defects preferably by using autografts which have to be donated and consequently harder to reach. Also there are many unsuccessful replacement experiments which increases the interest of cartilage tissue engineering to repair cartilage defects [3, 4, 5, 6].

### 2.3 Cartilage Tissue Engineering and Cell Based Therapies

Cartilage is an aneural and avascular tissue in which any damage to the tissue may not be able to repaired by itself and may lead to disability. Cell based therapies according to the principles of cartilage tissue engineering has been a great hope for a long term treatment of this tissue. There are three main elements to improve these techniques: cells, cell substrates and culture conditions [7]. Although some re-

searches have obtained good repair of cartilage defects for short terms, there are still a great need for the development of these techniques and eliminate the drawbacks by preparing novel biomaterials and searching for suitable cell sources for cartilage tissue engineering [3].

Autologous chondrocyte transplantation is one of the cartilage regeneration techniques in which chondrocytes are isolated from the healthy cartilage tissue of the patient, cultured and populated to have desired amount of cells and implanted to the damaged area. The biggest problem in this treatment is dedifferentiation of chondrocytes which is defined as loss in function, morphology, shape of chondrocytes and expression of fibroblast-like. Thus, implanted cells have lost their capacity to regenerate cartilage and the efficiency of the treatment is decreased. Also further treatments would be required to redifferentiate cells into chondrocytes [8].

Besides from dedifferentiation, donor site morbidity and chondrocyte supply problems are other important drawbacks of autologous cartilage transplantation [21, 22]. Therefore, researchers have been seeking for a new cell source for cartilage regeneration. Allogenic cells were thought to be used, however considering the possibility of immunological rejection during culture, the idea was dropped and the researchers concentrated on the use of mesenchymal stem cells (MSCs). Using MSCs show lower immunological reaction than adult cells [23, 24, 25]. Mesenchymal stem cells can be obtained from various tissues as bone marrow and adipose tissue. They can be isolated without any damage to donor and they have multiple differentiation capacity, self-renewal potential and also they can be accessed easily. In various cartilage regeneration studies, MSCs showed a better cell arrangement than adult chondrocytes. Cartilage repair with MSCs has been an actively studied topic. The studies showed certain success, however some researchers showed that, cartilage healing was slowed down after 1 month of transplantation. They also observed some degenerative changes in cartilage tissue [25]. Thus, further improvements are necessary for MSC based therapies with sustainable repair including adjusting the cell substrate properties to the micro-environment of cartilage.

Dedifferentiation of chondrocytes may come of many factors as cell type, cell substrate, rapid proliferation and exposure to some biochemical products. During cell culture, contact with a rigid, flat surface, which is highly different from cell's original

environment, promotes dedifferentiation the most. To avoid this, altering physical, mechanical and chemical properties of the cell culture environment is essential [8].

## 2.4 Effects of cell substrate properties on stem cell differentiation

Micro-environment of cells and biomolecular signals from their micro-environment orientate specific functions of cells. To carry out their unique functions, biochemical and biophysical inputs from microenvironment are very important. By mimicking these signals and preparing novel biomaterials in a precise and near-physiological fashion have attracted much interest. These mimic systems serve as a powerful cell substrates for stem cell differentiation [26].

In stem cells, biochemical composition of extra cellular matrix is not enough for controlling self-renewal and differentiation. Biomechanical forces, such as topography and substrate stiffness are crucial for modulating extracellular matrix features to change in shape and size [27]. Stiffness of the microenvironment may lead preferred differentiation of stem cells. For example, rigid cells resembling precalcified bone provide stem cells to an osteogenic differentiation. Also, it was shown in a study that collagen I-coated firm gels with muscle mimicked elasticity caused stem cells to upregulate myogenic markers [27].

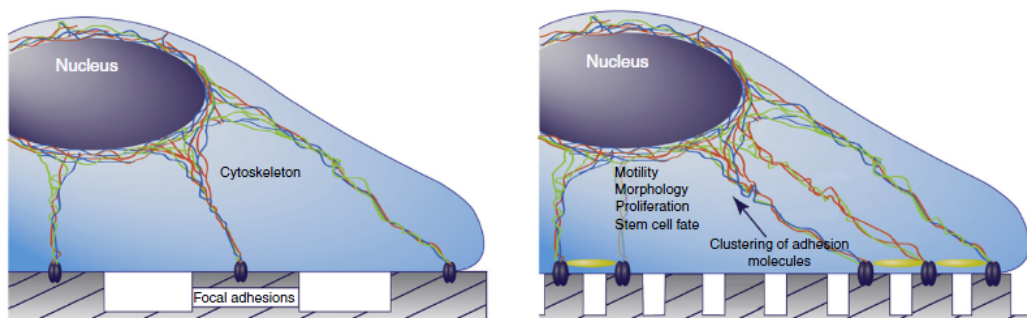


**Figure 2.5** Examples of topographical effects on cellular behaviour [11].

It has been proved [28, 29] that cells are sensitive to topographical properties

and change their behaviour accordingly to this input through focal adhesions (see Figures 2.5 and 2.6) [11]. Controlling physical conditions of the cell substrate is a novel approach to stem cell fate and differentiation. Cells and extracellular matrix are organised in a complex topographical features. Culturing stem cells on materials with extracellular matrix-like topography regulated stem cell differentiation, cell shape, proliferation and organization [29].

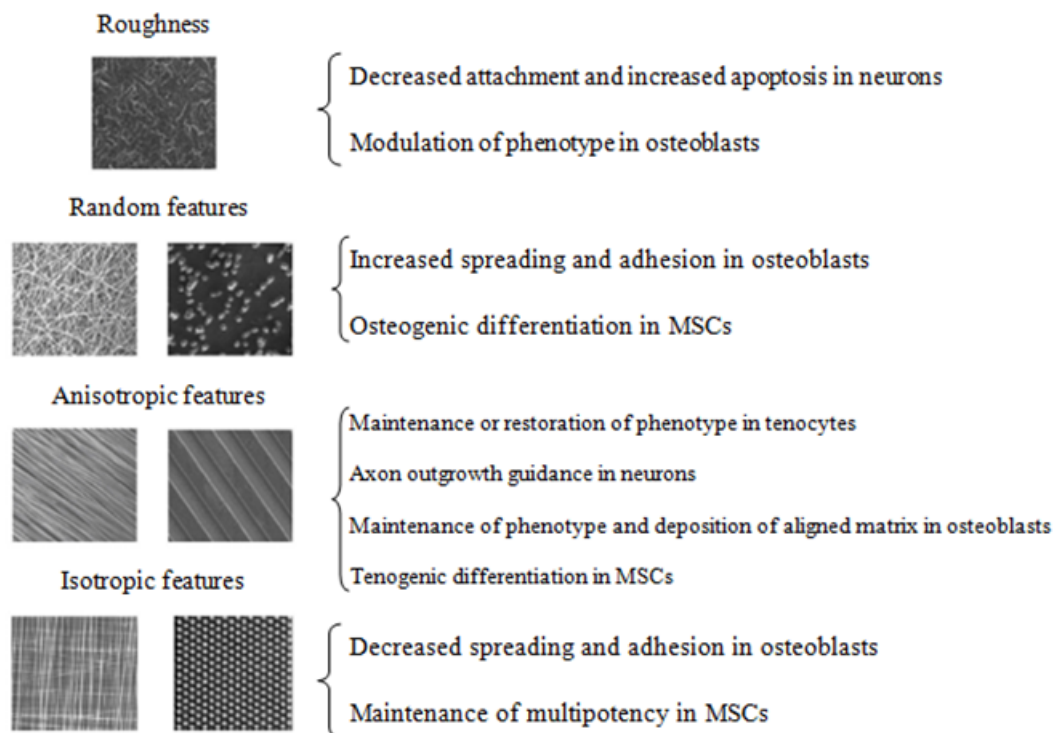


**Figure 2.6** Sensitivity of cells to surface topography through focal adhesions [11].

Several studies in tissue engineering have shown that surface chemistry has an important effect on cellular behaviour (adhesion, proliferation and fate) and stem cell differentiation [10, 30, 31, 32]. As the extracellular matrix of cartilage is primarily composed of water, proteoglycans, collagens, elastin, glycoproteins and interstitial fluid [1], functionalizing substrate's surface with extracellular matrix-like chemicals may improve cellular behaviour and promote chondrogenic stem cell differentiation.



## 2.5 Polymeric Materials for Cartilage Tissue Engineering and Polydimethylsiloxane

Many natural and synthetic polymers have been used to produce cell substrates for cartilage tissue engineering (see Table 2.1). Natural polymers which are economic, biodegradable, low toxic and renewable, are widely used as substrates in cartilage tissue engineering [32]. They send biological signals and have properties of cell adhesion and cell responsive degradation. However, they may lose their biological properties during substrate fabrication because of their tendency to rapid degradation. Also in substrates made from natural polymers, there is a risk of immunorejection and disease transmission [7, 32].

Physical, mechanical and chemical properties of synthetic polymers can be altered easily. Also they are easy to process into desired shape. These advantages of synthetic polymers enables their successful use in cartilage tissue engineering [7].

Polydimethylsiloxane (PDMS), a nontoxic, biocompatible, bioinert and Si based synthetic polymer, is a commonly used cell substrate, as its mechanical properties are easily altered. It is an elastomeric polymer composed of a pre-polymer and a cross-linker. Producing PDMS with different ratios of pre-polymer and cross-linker provides PDMS different stiffness' [33]. Since cells can feel stiffness and change their behavior according to this input, PDMS is a very convenient biomaterial for cell studies [27].

Cartilage regeneration with stem cell therapy requires a convenient substrate which mimicks the biochemical signals coming from the extracellular matrix [26]. As the extracellular matrix is primarily composed of water, proteoglycans, collagens, elastin, glycoproteins and interstitial fluid [1], functionalizing substrate's surface with extracellular matrix-like chemicals may promote this specific stem cell differentiation. As amino acids are building blocks of proteins, functionalizing the surface with them could provide cartilage extracellular matrix-like environment. Also, recent studies showed that, modifying cell substrate's surface with amino acids helps to reduce toxicity [34].

PDMS is a highly hydrophobic material and does not have any cell binding sites.

**Table 2.1**  
Natural and synthetic polymers used in cartilage tissue engineering [7].

Synthetic Polymers	Natural Polymers
Polyvinyl alcohol	Cellulose
Poly (L-lactide-co-3-caprolactone) (PLCL)	Collagen
Polyglycolic acid (PGA)	Hyaluronic acid
Polylactic acid(PLLA)	Dextrans
Polylactic-co-glycolic acid(PLGA)	Fibrin
Polyurethane	Chitosan
Polybutyric acid	Carboxymethyl chitosan
Polytetrafluorethylene	Alginate
Polyethyleneterephtalate	Agarose
Poly(N-isopropylacrylamide)	
Polyethylene glycol fumerate	
Polydimethylsiloxane (PDMS)	

Therefore, surface modifications are essential for cell adhesion. In order to make PDMS surface convenient for functionalization with some molecules and proteins, surface activation is required [33]. For the modification of PDMS with amino acids, self assembled molecules can be used. Self-assembling is a spontaneous organization of atoms and molecules into an ordered array of elements [15]. Monolayers can be formed by self assembly of some molecules. With these self assembled molecules, desired flexible design requirements and increased stability can be acquired [35].

## 3. MATERIALS AND METHODS

### 3.1 Surface Preparation

#### 3.1.1 Preparation of Plain PDMS Substrates

Polydimethylsiloxane was used as a substrate to mimic the micro-environment of the cartilage. Substrates were prepared by using the PDMS preparation kit (PDMS, Sylgard 184; Dow Corning, Midland, MI), composed of pre-polymer and cross-linking agent. To prepare substrates with different stiffness, amounts of pre-polymer and cross-linking agent were changed to be 10:1, 15:1, 20:1 and 30:1 (w/w). The components were mixed extensively and put in a vacuum chamber to remove bubbles. At first, degassing process was performed with short intervals. Then, after almost all of the bubbles were removed, the system was put under vacuum for 30 minutes approximately. After this step, PDMS was poured into aluminum plates and baked for 4 hours at 70°C [36].

Cured PDMS samples were peeled from the aluminum plates and cut by using a circular blade with a diameter of 1.5 cm. Then substrates were cleaned in an ultrasonic bath (Bandelin-Sonorex) first in ethanol and in distilled water, for 10 minutes each. Substrates were dried with N<sub>2</sub> gas.

#### 3.1.2 Preparation of Patterned PDMS Substrates

Surface topography of the PDMS substrates were prepared for controlling the architectural features of cartilage tissue. As type II collagen is the dominant collagen for cartilage tissue, bundles of the type II collagen were mimicked on PDMS substrates by soft-lithography technique [37]. To do this, a template was designed (according to TEM photos of collagen II fibers, see Figure 2.2) with various width, length and distances using photolithographic processing. The master geometry was shown in Figure 3.1 as horizontal period and size of line width was changed to be 100, 150, and 200  $\mu\text{m}$  (A),

size of line length was changed to be 30, 40 and 50  $\mu\text{m}$  (B), while the perpendicular period was changed to be 30, 40 and 50  $\mu\text{m}$  (C).

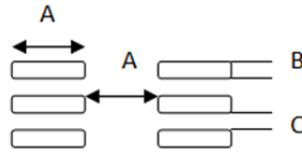


**Figure 3.1** Geometry and size of type II collagen bundles-like template.

**Table 3.1**  
Pattern dimensions of Collagen Type II bundles-like template

	A ( $\mu\text{m}$ )	B ( $\mu\text{m}$ )	C ( $\mu\text{m}$ )
a	100	30	30
b	100	30	40
c	100	30	50
d	100	40	40
e	150	30	30
f	150	30	40
g	150	40	40
h	150	40	40
i	200	30	30
j	200	30	40
k	200	30	50
l	200	40	40

Template was fabricated by using a single side polished silicon wafer, since the features were created on one side of the wafer. Preparation process was started with cleaning of the wafer by dipping it into acetone, isopropanol (IPA) and deionized water (DI) baths sequentially. Then the wafer was baked at 200°C for dehydration. For the lithography process, first the wafer was coated with the SU-8 2005 (MicroChem) photoresist by using spin coater in 1800 rpm for 40 sec and then soft baked at 95°C for

3 min. After cooling at room temperature, the wafer was exposed to UV light at 120 mJ/cm<sup>2</sup> by using mask aligner and then was post baked at 65°C for 1min, at 95°C for 3 min and at 65°C for 1 min. Finally, substrate was placed into the SU-8 developer solution for 7 min in order to remove unexposed photoresist. Then this silicon wafer was used as a mold. To prepare col II bundles-like patterns on PDMS substrates surfaces, PDMS mixtures with four different crosslink ratios (10:1, 15:1, 20:1 and 30:1) were degassed. A petri dish was covered with aluminum foil and the silicon wafer was placed on this dish. Degassed PDMS was poured on the template and put in an oven for 4h at 70°C. After curing, PDMS and the template were separated from the petri dish and PDMS replica was peeled from the template.

### **3.1.3 Chemical Modification of PDMS Substrates**

PDMS substrates were modified with amino acid conjugated self assembled monolayers and with (3-Aminopropyl)triethoxysilane (APTES) molecule.

#### **3.1.3.1 Modification of PDMS Substrates with APTES.**

Cleaned PDMS substrates were treated with oxygen (O<sub>2</sub>) plasma (March Plasma Systems, PM-100) to activate surfaces. Treatment was performed for 1 min at 200 mT and 50 sccm flow of oxygen to form hydroxyl groups on the PDMS surfaces [38] Aqueous solution of APTES (v/v, 1%) was prepared and PDMS substrates were dipped in the solution for 20 min at room temperature. After this reaction time, substrates were washed with distilled water and dried with an N<sub>2</sub> gas [38].

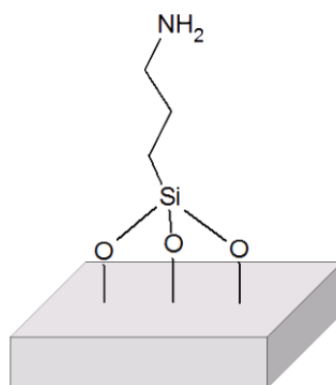
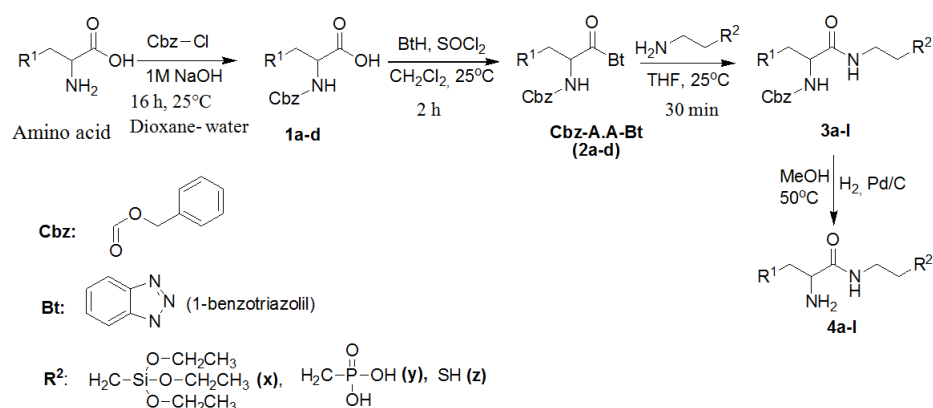


Figure 3.2 APTES modified PDMS.

### 3.1.3.2 Synthesis of Amino Acid Conjugated Self Assembled Molecules.

Dichloromethane ( $\text{CH}_2\text{Cl}_2$ ) was purified and used after boiling with sodium metal on calciumhydride ( $\text{CaH}_2$ ) with the presence of tetrahydrofuran (THF) benzophenone. Solution of amino acid (1 equivalent) in NaOH (aq, 1,5 equivalent) was cooled in an ice bath. Cbz-Cl's (1,3 equivalent) solution in dioxane was added to the amino acid solution drop by drop. Then, the reaction mixture was mixed at  $0^\circ\text{C}$  for 30 min and at room temperature for 16 h. After this time, dioxane was evaporated under vacuum and extracted with ethyl acetate (3x25 mL). pH of the liquid phase was fixed 2 by using 1M HCl. Acidified liquid phase was extracted by using ethyl acetate (4x20 mL). Organic phase was was dried with sodiumsulphate and by evaporating the solvent under vacuum, amino acids, Cbz-Leu-Bt, Cbz-Trp-Bt, and Cbz-His-Bt, were synthesized [36].

Characterization of His-SAM, Leu-SAM and Trp-SAM was done by using NMR spectroscopy (Bruker, 500 MHz, Germany) in  $\text{CDCl}_3$  or DMSO-d6. Tetramethylsilane was used as internal standard.



**Figure 3.3** General synthesis procedure for the amino acid conjugated self assembled molecules.

### 3.1.3.3 Modification of PDMS Substrates with SAMs.

PDMS substrates were cleaned and modified with amino acid conjugated self assembled molecules (Histidine-SAM, Leucine-SAM and Tryptophan-SAM). PDMS substrates were dipped in amino acid conjugated SAMs to investigate the effects of concentration (1-20 mM) and dipping time (1h-24h) on the formation of the self assembled monolayers. After the reaction time, PDMS substrates were rinsed with ethanol and dried with  $\text{N}_2$  gas.

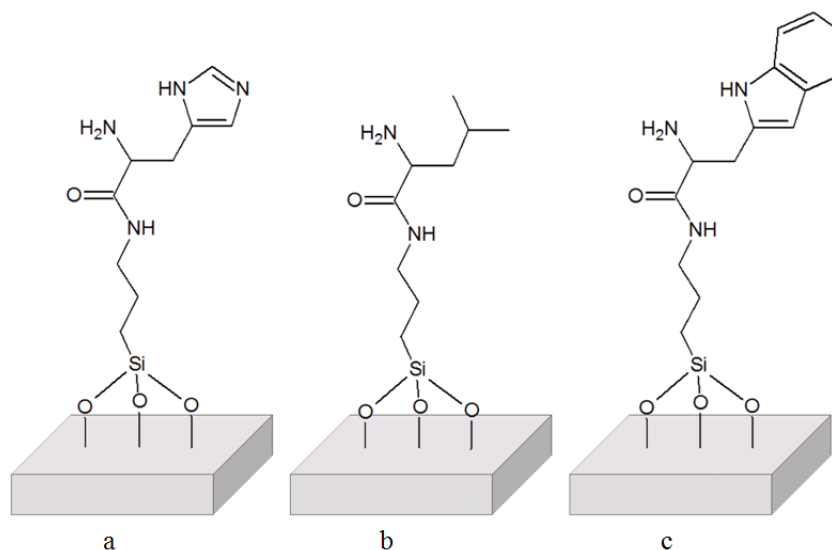


**Figure 3.4** Amino acid conjugated SAMs on PDMS substrate a) His-SAM, b) Leu-SAM, c) Trp-SAM.

### **3.1.3.4 Modification of PDMS Substrates with Type II Collagen.**

PDMS substrates were sonicated in ethanol and distilled water for 10 min each. PDMS surface was activated by oxygen plasma treatment (March Plasma Systems, PM-100) for 1 min at 200 mT and 50 sccm flow of oxygen to form hydroxyl groups on the PDMS surfaces [38].  $\text{NH}_2$  Activated PDMS surface were modified with APTES (v/v, 1%) to create amino ( $-\text{NH}_2$ ) groups for 20 min at room temperature (RT). Then PDMS substrates with amino groups were immersed in 1% glutaraldehyde solution for 3h at RT. After the reaction time, substrates were washed with distilled water extensively and dried with  $\text{N}_2$ . 0.1mg/mL aqueous Collagen II solution including 0,3% acetic acid was prepared and mixed at RT until Collagen II was completely dissolved. Then the solution was poured on glutaraldehyde modified PDMS substrates for 24h at 4°C. Substrates were washed extensively with distilled water and dried with  $\text{N}_2$  gas [39].

## **3.2 Surface Characterization**

### **3.2.1 Characterization of Mechanical Properties of PDMS Substrates**

PDMS substrates' elastic modulus with four different pre-polymer and cross-linking agent ratios (10:1, 15:1, 20:1 and 30:1), were measured using a nanoindenter (CellHesion<sup>®</sup>200, JPK, Germany). Young' moduli of the substrates were provided by using Hertz model after measurements. The indentation measurements were performed in contact mode, using a CONT cantilever (Nanoworld, contact mode afm probes) which has a pyramidal tip made of monolithic silicon with a force constant of 0.2 N/m and resonance frequency of 13 kHz [40].

Young's modulus is an elastic property, which is a measure of stiffness - the higher Young's modulus value, the stiffer material. Young's modulus is given by the equation 3.1:



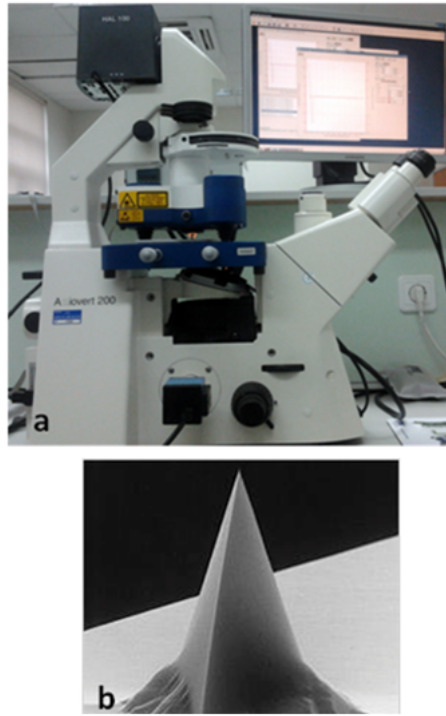


**Figure 3.5** a) CellHesion<sup>®</sup>200, b) Pyramidal tip of a CONT cantilever.

$$E = \frac{F.L}{\Delta L.A} \quad (3.1)$$

For data acquisition, firstly force calibration of the system was done by using a glass slide. Then sample was placed on the sample holder and mechanical data was acquired with an extend speed of  $5 \mu\text{m/s}$  and sample rate of 2000 Hz. Pulling length was adjusted according to the stiffness of the sample. PDMS substrates with higher cross-linking agent ratios, pulling length was selected to be  $2 \mu\text{m}$  and with decreasing amount of cross-linking agent, pulling length was adjusted to be higher values as  $10 \mu\text{m}$ . Mechanical data acquisition was performed on three different areas of three different PDMS substrates for all different pre-polymer and cross-linking agent ratios (10:1, 15:1, 20:1 and 30:1) and three force measurements were carried out each time. With this mechanical data, Young's modulus calculations were done by using CellHesion<sup>®</sup>200 software according to the Hertz model.

### 3.2.2 Characterization of Patterned PDMS Substrates

Patterned PDMS substrates were characterized by using optical microscopy. Substrates were cut by using a circular blade with a diameter of 1.5 cm. Then substrates were cleaned in an ultrasonic bath (Bandelin-Sonorex) first in ethanol and in distilled water, for 10 minutes each. Substrates were dried with N<sub>2</sub>. Then, optical images were recorded by an optical microscopy (Leica, DTC295).

### 3.2.3 X-ray Photoelectron Spectroscopy (XPS)

To examine the changes in chemical composition of PDMS substrates, XPS (Thermo Scientific K-Alpha X-ray Photoelectron Spectrometer) was used. Analysis were performed using monochromated aluminum K $\alpha$  radiation, at 72 W, 400  $\mu$ m spot size, 90° angle and with a 128-channel detector.

### 3.2.4 Contact Angle Measurements

Wettability of bare and modified PDMS substrates were investigated by using contact angle measurements (CAM 100, KSV). Measurements were performed at room temperature with fixed amount of distilled water drop (approximately 6  $\mu$ m drop diameter) and 10 images were taken with 1 s time intervals. After recording the data, by using the software of the device, contact angles were calculated. Contact angle measurements were performed from 3 different areas of 3 samples for each of the bare and modified (APTES, amino acid conjugated SAMs, type II collagen) substrates.

## 4. RESULTS

### 4.1 Nanoindentation Measurements of PDMS Substrates

Young's moduli of PDMS substrates with different prepolymer/crosslinker ratios (w/w; 10:1, 15:1, 20:1 and 30:1) were measured by using Hertz model and shown in the Figure 4.1. According to the measurements, Young's moduli of 10:1, 15:1, 20:1 and 30:1 PDMS were found to be  $2.13\pm 0.15$  MPa,  $1.47\pm 0.07$  MPa,  $0.72\pm 0.05$  MPa and  $0.56\pm 0.06$  MPa respectively.

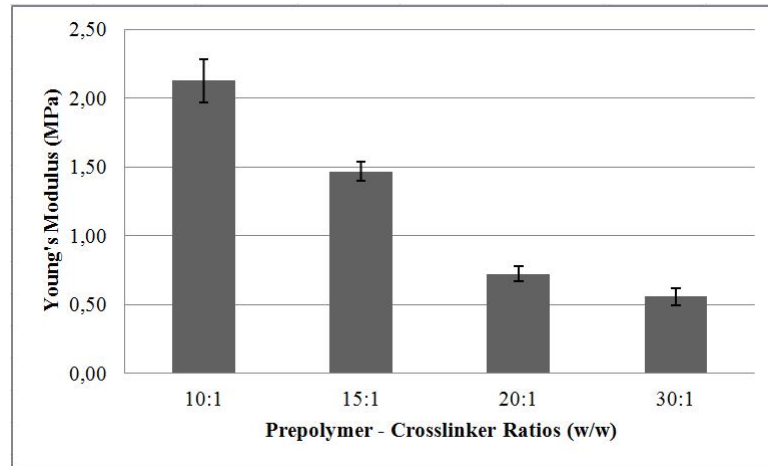


**Figure 4.1** Young's moduli data of PDMS, w/w; prepolymer-crosslinker ratio. Measured with CellHesion<sup>®</sup>200 by using Hertz model, in air, at 25°C,  $p < 0.0001$ .

### 4.2 Optical Microscopy

Collagen type II fibers alignment in human adult cartilage tissue was mimicked on PDMS surface by using soft lithography process. A template was designed according to Transmission electron microscopy (TEM) photo of type II collagen fibers of human cartilage with various dimensions (see Table 3.1). Surface topography of type II collagen bundles-like patterned PDMS substrates were analyzed by using optical microscopy and they were shown in the Figure 4.2. From these optical microscopy

images, the template topography was shown to be mimicked properly with PDMS for all different dimensions.

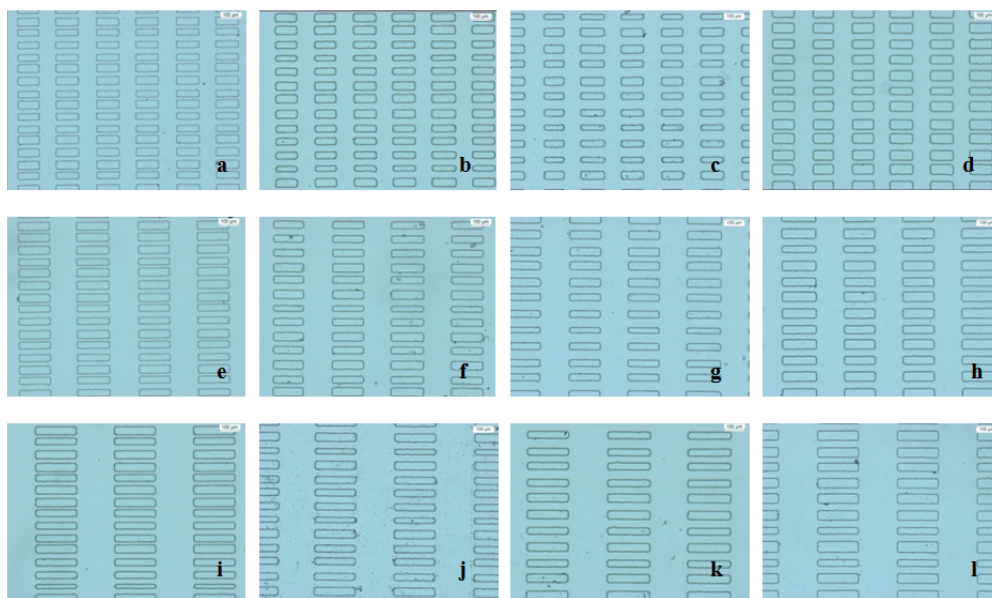


**Figure 4.2** Surface patterning on PDMS substrate (for dimensions see Table 3.1).

### 4.3 Characterization of Amino Acid Conjugated Self Assembled Molecules

After the reactions for the production of His-SAM, Leu-SAM and Trp-SAM, for Leu-SAM; white microcrystals were obtained with 78% yield. For Trp-SAM and for His-SAM, white microcrystals were obtained with 91% yield. yellow oil was produced with 87% yield. After the reaction for His-SAM, nonisolated byproducts were obtained. This product's mixture was reacted with amies directly and Nuclear Magnetic Resonance (NMR) analysis were done from this mixture.

Characterization of His-SAM, Leu-SAM and Trp-SAM was done by using NMR spectroscopy (Bruker, 500 MHz, Germany) in  $\text{CDCl}_3$  or  $\text{DMSO-d}_6$ . Tetramethylsilane was used as internal standard. NMR spectra of His-SAM, Leu-SAM and Trp-SAM were found in Figure 4.3, Figure 4.4 and Figure 4.5

For His-SAM,  $^1\text{H}$  NMR (500 MHz,  $\text{DMSO-d}_6$ ):  $\delta = 9.13$  (s, 1H), 8.54 (d, J =

7.2 Hz, 1H), 8.30 (q, J = 8.3 Hz, 2H), 7.82-7.87 (m, 1H), 7.65-7.70 (m, 1H), 7.54 (s, 1H), 7.30-7.37 (m, 5H), 5.88 (q, J = 8.3 Hz, 1H), 5.06 (s, 2H), 3.46-3.50 (m, 1H), 3.35-3.43 (m, 1H).

For Leu-SAM,  $^1\text{H-NMR}$  (500 MHz,  $\text{CDCl}_3$ ):  $\delta$  8.30 (d, J = 8.23 Hz, 1H), 8.15 (d, J = 8.23 Hz, 1H), 7.69 (t, J = 7.25 Hz, 1H), 7.55 (t, J = 7.25 Hz, 1H), 7.42-7.34 (m, 5H), 5.87 (dt, J = 8.29, 4.88 Hz, 1H), 5.51 (d, J = 8.49 Hz, 1H), 3.70 (s, 2H), 2.00-1.70 (m, 3H), 1.15 (d, J = 5.34 Hz, 3H), 1.00 (d, J = 5.34 Hz, 3H) ppm

For Trp-SAM,  $^1\text{H NMR}$  ( $\text{CDCl}_3$ ):  $\delta$  = 11.00 (s, 1H, NH-Trp), 8.00 (s, 1H, NH), 7.60-7.50 (m, 1H, Trp-H), 7.30 (d, 1H, J = 7.80 Hz, Trp-H), 7.20 (s, 1H, Trp-H), 7.10-6.90 (m, 2H, Trp-H), 3.50 (s, 9H,  $(\text{OCH}_3)_3$ ), 3.30-2.90 (m, 3H, NH- $\text{CH}_2$ ), 2.80-2.60 (m, 2H,  $-\text{CH}_2-$ ), 1.80-1.40 (m, 2H,  $-\text{CH}_2-$ ), 0.80-0.50 (m, 2H, Si- $\text{CH}_2-$ ) ppm.

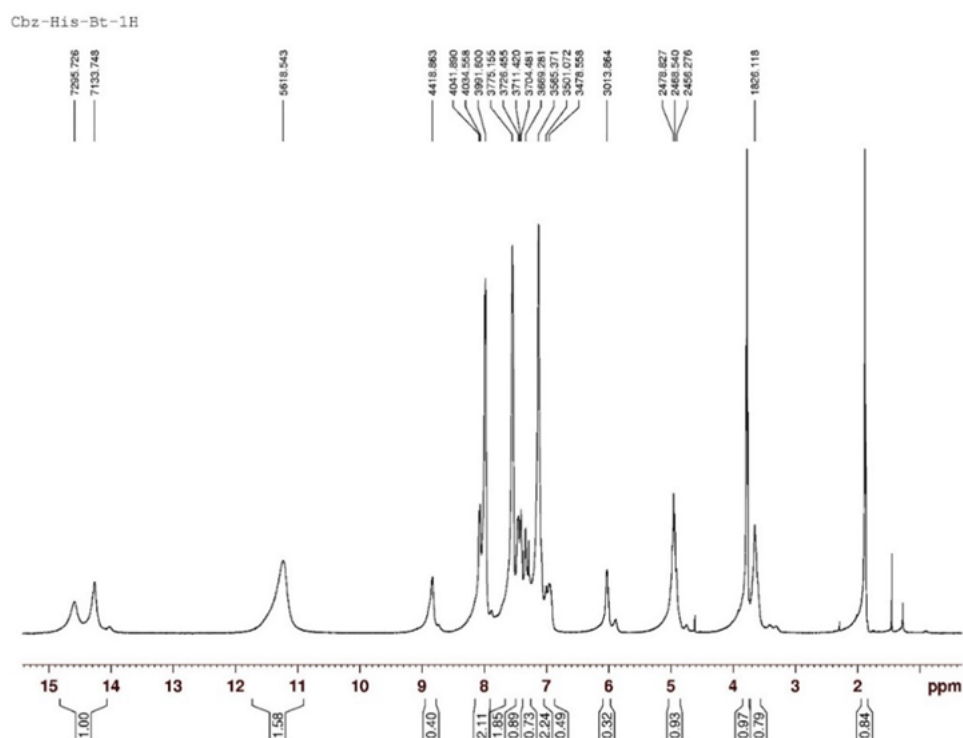
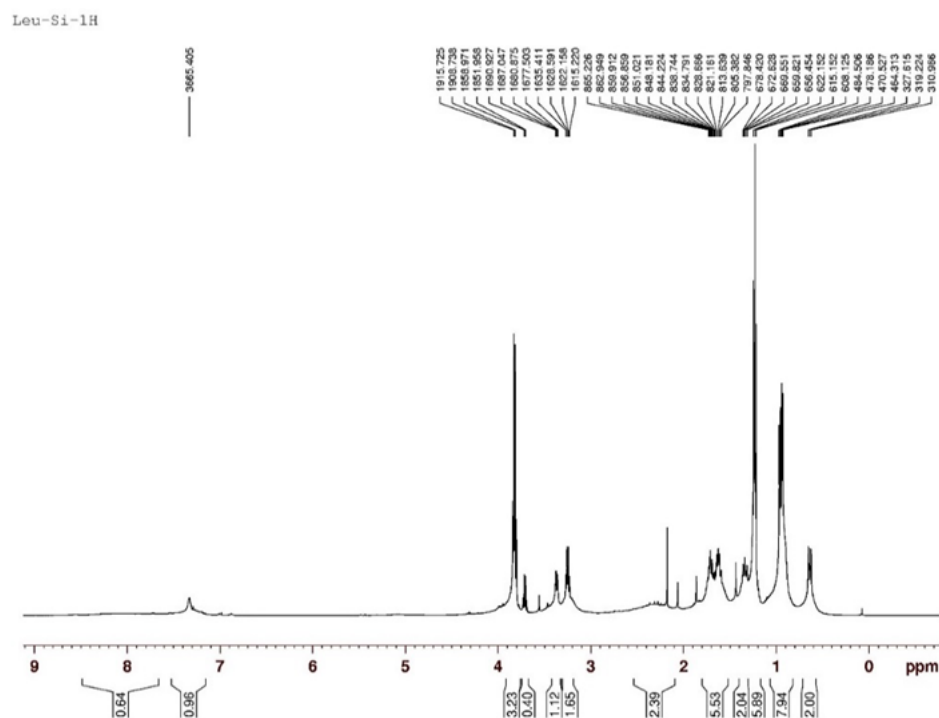


**Figure 4.3**  $^1\text{H NMR}$  spectrum of His-SAM (Benzyl 1-(1H-benzo[d][1,2,3]triazol-1-yl)-3-(1H-imidazole-4-yl)-1-oxopropane-2-ylcarbamate).



## 4.4 Contact Angle Measurements

### 4.4.1 Contact Angle Measurements of Bare PDMS Substrates with Different Prepolymer/Cross linker Ratios

Contact angles of bare PDMS substrates prepared with different prepolymer/cross linker ratios (w/w; 10:1, 15:1, 20:1 and 30:1) were measured by using CAM 100, USA and shown in the Table 4.1. After the measurements, contact angles were calculated to be  $104.10 \pm 5.12^\circ$ ,  $105.57 \pm 5.66^\circ$ ,  $109.13 \pm 3.73^\circ$  and  $107.74 \pm 5.30^\circ$  for the PDMS substrates having prepolymer/ cross linker ratios of 10:1, 15:1, 20:1 and 30:1, respectively. According to the figure, changing the prepolymer/cross linker ratios (w/w; 10:1, 15:1, 20:1 and 30:1) slightly changed PDMS substrate's wettability. Captured photos of the water drops on the PDMS surfaces with different prepolymer/crosslinker ratios were presented for 10:1, 15:1, 20:1 and 30:1 in Figure 4.6.

**Table 4.1**

Contact angle measurements of Bare PDMS with different pre polymer-crosslinker ratios.

Prepolymer-crosslinker ratio(w/w)	Contact Angle ( $^\circ$ )	Standard Deviation
10:1	104.10	5.12
15:1	105.57	5.66
20:1	109.13	3.73
30:1	107.74	5.30

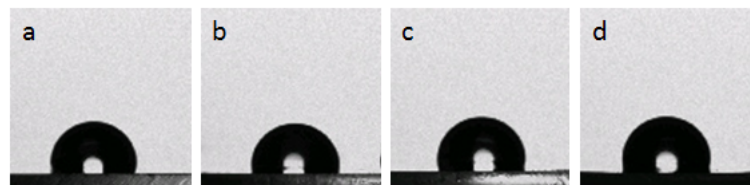


**Figure 4.6** Captured photos of the water drops on the PDMS surfaces with different prepolymer/ cross linker ratios (w/w) a) 10:1, b) 15:1, c) 20:1, and d) 30:1.

#### 4.4.2 Contact Angle Measurements of Bare and APTES (1% v/v) Modified PDMS Substrates

Contact angles of bare and APTES (1% v/v) modified PDMS substrates prepared with a prepolymer/ cross linker ratio of 10:1 (w/w) were measured by using CAM 100, USA and shown in the Table 4.2. After the measurements, contact angles were calculated to be  $104.10 \pm 5.12^\circ$  and  $61.98 \pm 5.51^\circ$  for bare and APTES (1% v/v) modified PDMS substrates. According to the figure, APTES (1% v/v) modification caused the PDMS surface to be hydrophilic. Captured photos of the water drops on the bare and APTES (1% v/v) modified PDMS surfaces were presented in Figure 4.7.

**Table 4.2**  
Contact angle measurements of Bare and APTES modified PDMS substrates.

	Contact Angle ( $^\circ$ )	Standard Deviation
PDMS, bare	104.10	5.12
PDMS, APTES modified	61.98	5.51

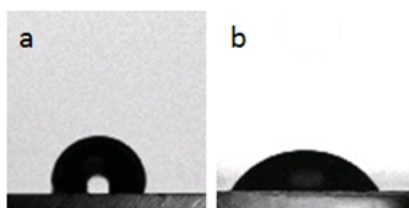


**Figure 4.7** Captured photos of the water drops on a) bare and b) APTES modified PDMS.

#### 4.4.3 Contact Angle Measurements of His-SAM Modified PDMS Substrates

PDMS substrates were modified with different concentrations of His-SAM (1-20 mM). Contact angles of PDMS substrates (prepolymer/crosslinker ratio of 10:1 (w/w))



with increasing concentrations (1-20 mM) of His-SAM modifications were measured by using CAM 100, USA and shown in the Table 4.3. After the measurements, contact angles were calculated to be  $100.89 \pm 6.79^\circ$ ,  $96.21 \pm 5.89^\circ$ ,  $91.30 \pm 5.56^\circ$ ,  $98.99 \pm 4.44^\circ$  and  $94.95 \pm 2.58^\circ$  for the His-SAM concentrations of 1 mM, 2 mM, 5 mM, 10 mM and 20 mM, respectively. Captured photos of the water drops on different concentration of His-SAM modifications on PDMS surfaces were shown in the Figure 4.7.

**Table 4.3**

Contact angle measurements of His-SAM modified PDMS substrates with different concentration (1-20mM) and dipping time:2h; in air, at 25°C.

Concentration	Contact Angle ( $^\circ$ )	Standard Deviation
1 mM	100.89	6.79
2 mM	96.21	5.89
5 mM	91.30	5.56
10 mM	98.99	4.44
20 mM	94.95	2.58

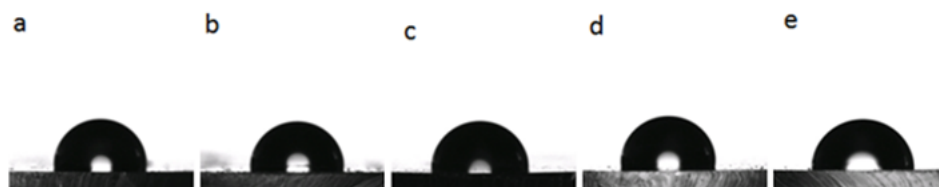


**Figure 4.8** Captured photos of the water drops on His-SAM modified PDMS substrates a) 1mM, b) 2 mM, c) 5 mM, d) 10 mM, e) 20 Mm.

PDMS substrates were modified with different dipping times of His-SAM. Effects of dipping time (1h-24h) on contact angles of PDMS substrates [prepolymer/cross linker ratio of 10:1 (w/w)] with 10 mM His-SAM modifications were investigated by using CAM 100, USA and shown in the Table 4.4. After the measurements, contact angles were calculated to be  $90.20^\circ \pm 6.03$ ,  $98.99^\circ \pm 4.44$ ,  $84.06^\circ \pm 5.92$  and  $101.17^\circ \pm 3.31$  for the corresponding dipping times of 1 h, 2 h, 4 h and 24 h, respectively. Captured photos for the investigation of the effect of dipping time on His-SAM modifications of PDMS

surfaces were shown in the Figure 4.9.

**Table 4.4**  
Contact Angle Measurements of His-SAM modified PDMS substrates with different dipping time (1-24h), His-SAM Concentration: 10 mM; in air, at 25°C.

Dipping time	Contact Angle (°)	Standard Deviation
1 h	90.20	6.03
2 h	98.99	4.44
4 h	84.06	5.92
24 h	101.17	3.31

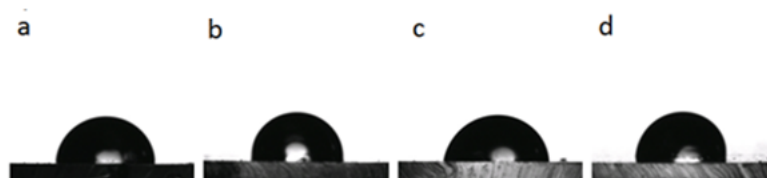


**Figure 4.9** Captured photos of the water drops of His-SAM (10mM) modified PDMS substrates; A) 1h, b) 2h, C) 4h, D) 24h.

#### 4.4.4 Contact Angle Measurements for His-SAM, Leu-SAM, Trp-SAM and Collagen type II Modified PDMS Substrates

PDMS substrates prepared with a prepolymer/crosslinker ratio of 10:1 (w/w) were modified with 10 mM His-SAM, Leu-SAM, Trp-SAM and 0,1mg /mL of type II collagen. Contact angles of PDMS substrates (prepolymer/ cross linker ratio of 10:1 (w/w)) modified with His-SAM, Leu-SAM, Trp-SAM and Collagen type II were measured by using CAM 100, USA and shown in the Table 4.5. After the measurements, contact angles were calculated to be  $93.51^{\circ} \pm 45.95$ ,  $86.76^{\circ} \pm 8.12$ ,  $93.83^{\circ} \pm 6.47$  and  $92.88^{\circ} \pm 8.78$  for His-SAM, Leu-SAM, Trp-SAM and Collagen type II modifications of PDMS substrates. Captured photos of the water drops on His-SAM, Leu-SAM, Trp-SAM and Collagen type II modifications of PDMS substrates were shown in the Figure 4.10.

**Table 4.5**

Contact Angle Measurements of His-SAM modified PDMS substrates with different dipping time (1-24h), His-SAM Concentration: 10 mM; in air, at 25°C.

Type of Modification	Contact Angle (°)	Standard Deviation
His-SAM	93.51	5.95
Leu-SAM	86.76	8.12
Trp-SAM	93.83	6.47
Col type II	92.88	8.78

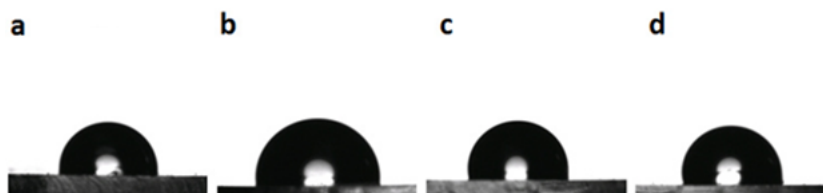


**Figure 4.10** Contact Angle Measurements for His-SAM, Leu-SAM, Trp-SAM and Collagen type II Modified PDMS Substrates; SAM concentration 10 mM; dipping time 2h, in air, at 25°C.

## 4.5 X-ray Photoelectron Spectroscopy (XPS) Analysis

### 4.5.1 XPS Analysis of Bare PDMS

Survey spectrum of bare PDMS was shown in Figure 4.11. XPS survey of bare PDMS showed Si2p, C1s and O1s peaks. In the analysis of Si2p core level, presence of Si-C and Si-O peaks were found at 102.1 and 103.7 eV, respectively [41]. In O1s core level, Si-O bond is shown at 532.7 eV [42]. C-Si bond was found in the C1s spectrum at approximately 284.6 eV [42].

Atomic percentages of the PDMS components (C, O, Si) were calculated from the area under the curves, as 46.79, 24.74 and 28.48% for C, O and Si atoms, respectively. Comparison of measured atomic percentages with theoretical ones were shown in the Table 4.6.

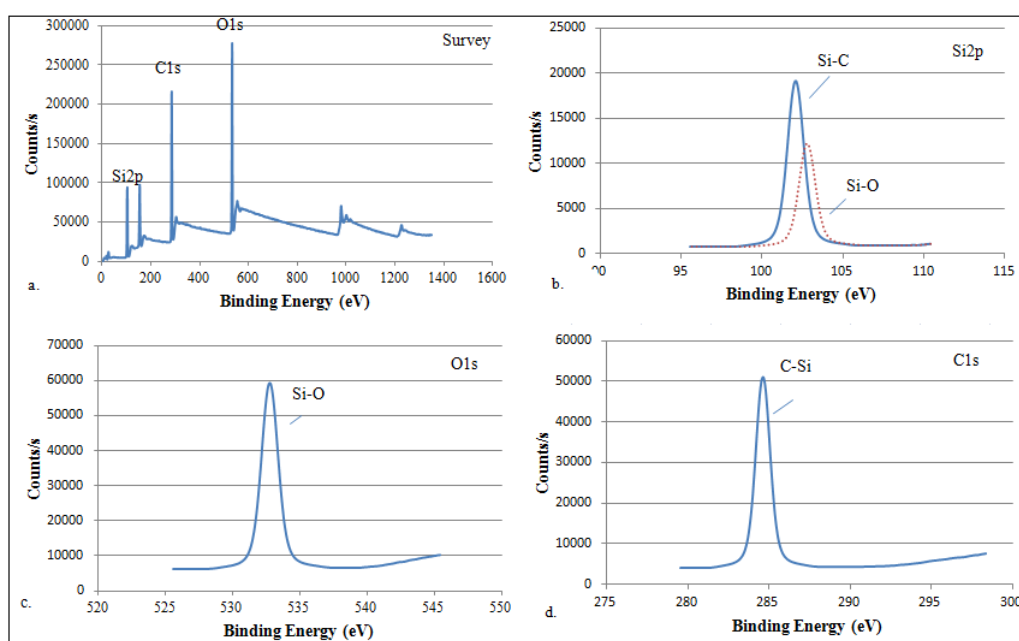


**Figure 4.11** XPS spectra of bare PDMS with survey spectrum, Si2p, O1s, and C1s regions.

**Table 4.6**

Theoretical and measured atomic percentages of C, O and Si atoms found in PDMS.

Atoms	Theoretical Atomic %	Measured Atomic %
C	50.00	46.79
O	25.00	24.74
Si	25.00	28.48

#### 4.5.2 XPS analysis of APTES modified PDMS substrates

XPS survey spectrum of APTES (1% v/v) modified PDMS substrates were shown in the Figure 4.12. According to the figure, Si2p, C1s, N1s and O1s peaks are found from the analysis.

XPS analysis for Si2p, C1s, O1s and N1s levels of APTES (1% v/v) modified PDMS substrates prepared with a prepolymer/ cross linker ratio of 10:1 (w/w) were measured by using Thermo Scientific K-Alpha XPS and shown in the Figure 4.13. As seen from the figure, Si-C and Si-O bonds were found in Si2p region at 101.8 and 103.4

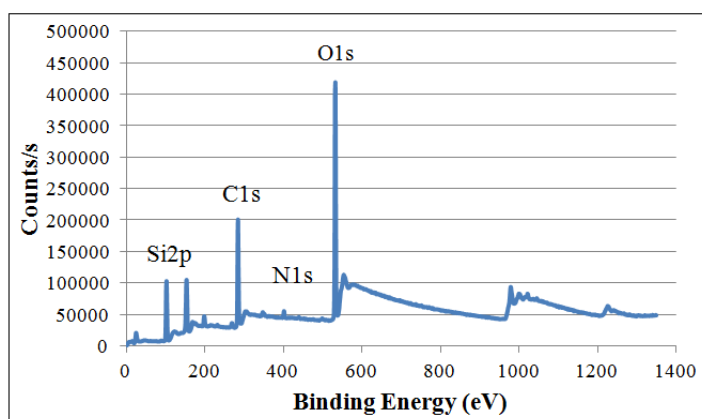


**Figure 4.12** XPS survey spectrum of APTES modified PDMS substrate.

eV [42]. In C1s core level; peaks were found at 284.4, 285.6 and 288.3 eV corresponding to C-Si, C-C and C-N bonds [42, 43, 44]. In O1s level, Si-O bond was shown at 532.1 eV and in N1s level, C-N bond was found at 401.8 eV [45].

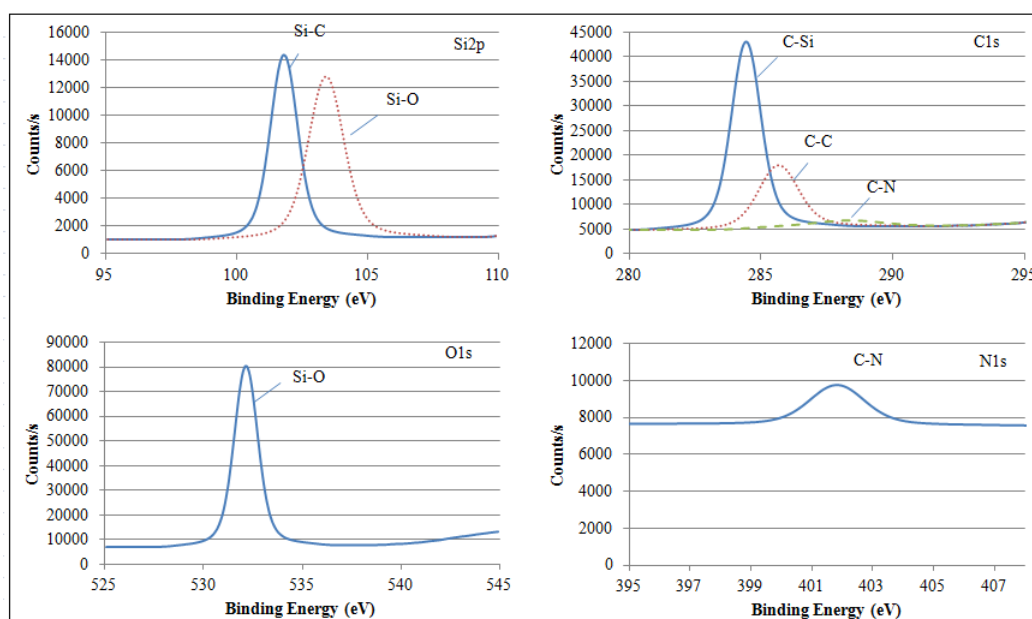


**Figure 4.13** XPS spectra of APTES modified PDMS with Si2p, C1s, O1s and N1s.

Atomic percentages of the APTES modified PDMS components (C, O, N, Si) were calculated from the area under the curves, as 38.00, 34.14, 1.65 and 26.22% for C, O, N and Si atoms, respectively. Comparison of measured atomic percentages with theoretical ones were shown in the Table 4.7.

**Table 4.7**

Theoretical and measured atomic percentages of C, O, N and Si atoms found in APTES modified PDMS substrates.

Atoms	Theoretical Atomic %	Measured Atomic %
C	35.00	38.00
O	35.00	34.14
N	5.90	1.65
Si	24.00	26.22

#### 4.5.3 XPS Analysis of His-SAM Modified PDMS Substrates

PDMS substrates were modified with different concentrations of Histidine conjugated self assembled molecules. XPS analysis of PDMS substrates [prepolymer/crosslinker ratio of 10:1 (w/w)] with increasing concentrations (1-20 mM) of His-SAM modifications were done by using Thermo Scientific K-Alpha XPS. In Table 4.8 theoretical and experimental atomic percentages of PDMS substrate modifications with different His-SAM concentrations were shown and according to these values, PDMS substrate surface was modified the most with 10 mM His-SAM.

**Table 4.8**

Theoretical and measured atomic percentages of C, O, N and Si atoms found in modified PDMS substrate different His-SAM concentration (1-20mM).

	Theoretical	1 mM	2 mM	5 mM	10 mM	20 mM
C	44.44	36.34	20.50	35.03	38.00	33.81
O	25.93	46.33	60.80	33.62	32.93	35.99
N	14.81	1.31	2.44	2.73	3.41	2.71
Si	14.81	16.01	16.25	28.60	25.86	27.46

PDMS substrates were modified with different dipping times of Histidine conjugated self assembled molecules. XPS analysis of PDMS substrates (prepolymer/crosslinker

ratio of 10:1 (w/w)) with increasing dipping times (1h-24h) of His-SAM modifications were done by using Thermo Scientific K-Alpha XPS. In Table 4.9 theoretical and experimental atomic percentages of PDMS substrate modifications with different His-SAM dipping time were shown.

**Table 4.9**

Theoretical and measured atomic percentages of C, O, N and Si atoms found in modified PDMS substrate with different dipping time of His-SAM (1h-24h).

	Theoretical	1 h	2 h	4 h	24 h
C	44.44	35.56	38.00	34.70	38.86
O	25.93	34.67	32.93	34.90	31.20
N	14.81	3.05	3.41	2.70	4.69
Si	14.81	26.72	25.86	27.80	25.26

XPS survey spectrum of His-SAM (10mM, 2h) modified PDMS substrates were shown in the Figure 4.14 According to the figure, Si2p, C1s, N1s and O1s peaks were obtained from the analysis.

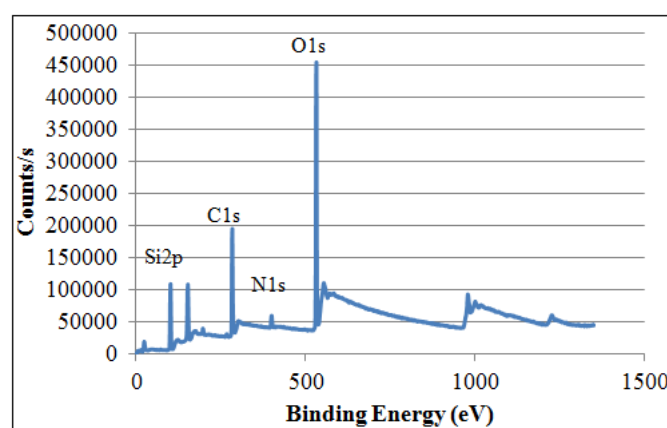


**Figure 4.14** XPS survey spectrum of His-SAM (10mM) modified PDMS substrate.

XPS analysis for Si2p, C1s, O1s and N1s core levels of His-SAM (10mM) modified PDMS substrates prepared with a prepolymer/ cross linker ratio of 10:1 (w/w) were measured by using Thermo Scientific K-Alpha XPS and shown in the Figure 4.15.

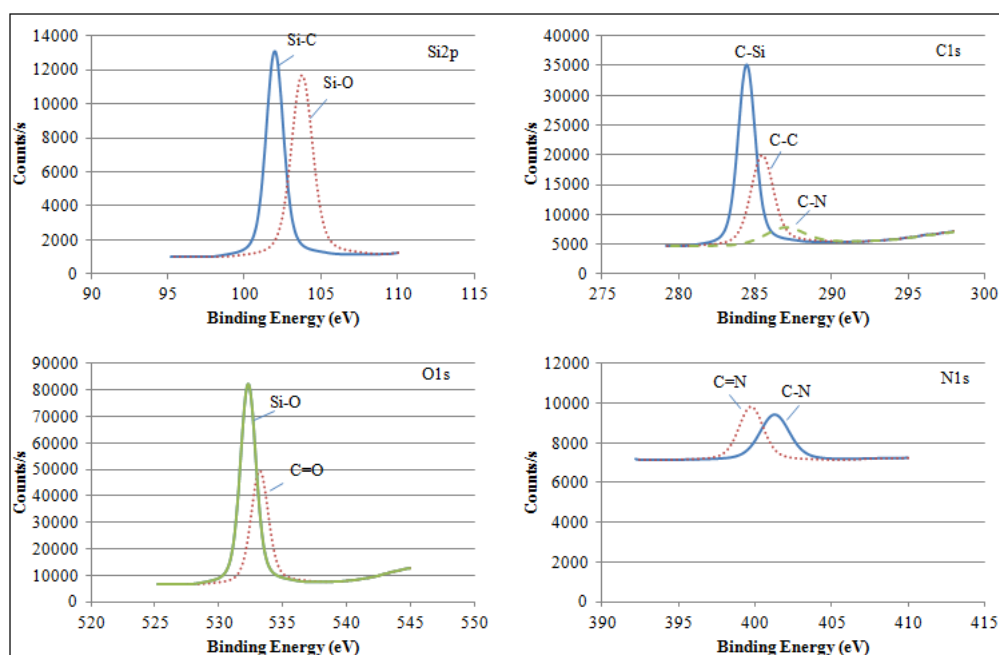


**Figure 4.15** XPS spectra of His-SAM (10mM) modified PDMS with Si2p, C1s, O1s and N1s regions.

As seen from the figure, Si-C and Si-O bonds were found in Si2p region at 102.0 and 103.6eV [41]. In C1s core level; peaks were found at 284.6, 285.9 and 288.2 eV corresponding to C-Si, C-C and C-N bonds [42, 43, 44]. In O1s level, Si-O bond was shown at 532.1 eV and in N1s level, C-N bond was found at 401,3 eV [42, 45].

#### 4.5.4 XPS analysis of Leu-SAM modified PDMS substrates

XPS analysis of Leu-SAM(10mM, 2h) modified PDMS substrates [prepolymer/cross linker ratio of 10:1 (w/w)] were done by using Thermo Scientific K-Alpha XPS. XPS survey spectrum of Leu-SAM (10 mM, 2h) modified PDMS substrates were shown in the Figure 4.16. According to the figure, Si2p, C1s, N1s and O1s peaks were obtained from the analysis.

XPS analysis for Si2p, C1s, O1s and Ni1s core levels of Leu-SAM (10mM, 2h) modified PDMS substrates were measured by using Thermo Scientific K-Alpha XPS and shown in the Figure 4.17. As seen from the figure, Si-C and Si-O bonds were



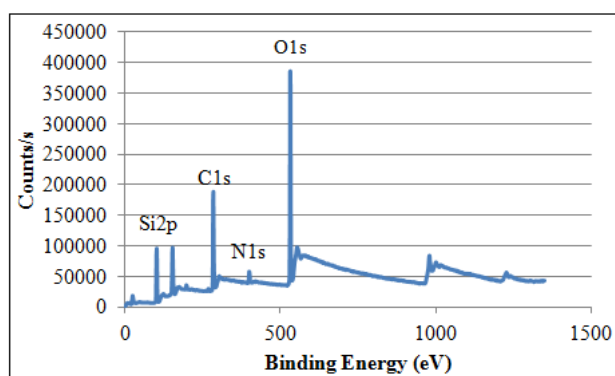


**Figure 4.16** XPS survey spectrum of Leu-SAM (10mM, 2h) modified PDMS substrate.

found in Si2p region at 101.9 and 103.0 eV [41]. In C1s core level; peaks were found at 285.2, 284.4, 286.3 and 288.2 eV corresponding to C-Si, C-C, C=O and C-N bonds [42, 43, 44, 46]. In O1s level, Si-O, C=O bonds was shown at 532.1 and 532.9 eV, and in N1s level, C-N bond was found at 400.0 eV [42, 46].

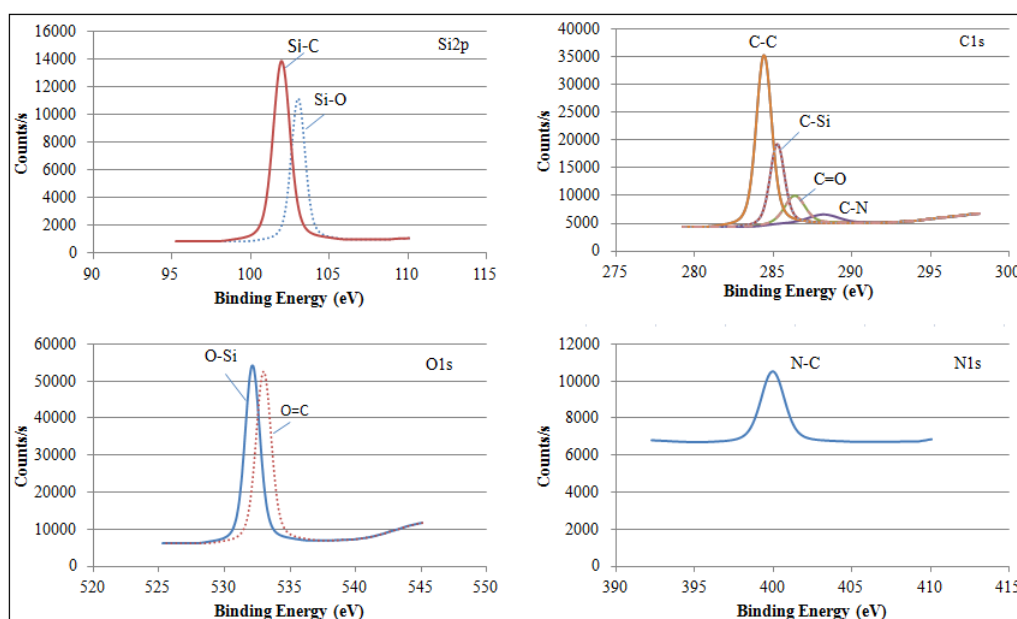


**Figure 4.17** XPS spectra of Leu-SAM (10mM,2h) modified PDMS with Si2p, C1s, O1s and N1s regions.

Atomic percentages of the Leu-SAM modified PDMS components (C, O, N, Si) were calculated from the area under the curves, as 38.36, 32.32, 3.36 and 25.96% for C, O, N and Si atoms, respectively. Comparison of measured atomic percentages with

theoretical ones were shown in the Table 4.10.

**Table 4.10**

Theoretical and measured atomic percentages of C, O, N and Si atoms found in Leu-SAM modified PDMS.

	Theoretical Atomic %	Measured Atomic %
C	50.00	38.36
O	25.00	32.32
N	8.33	3.36
Si	16.67	25.96

#### 4.5.5 XPS analysis of Trp-SAM modified PDMS substrates

XPS analysis of Trp-SAM(10mM, 2h) modified PDMS substrates prepolymer/crosslinker ratio of 10:1 (w/w)) were done by using Thermo Scientific K-Alpha XPS. XPS survey spectrum of Leu-SAM (10 mM, 2h) modified PDMS substrates were shown in the Figure 4.18. According to the figure, Si2p, C1s, N1s and O1s peaks were obtained from the analysis.

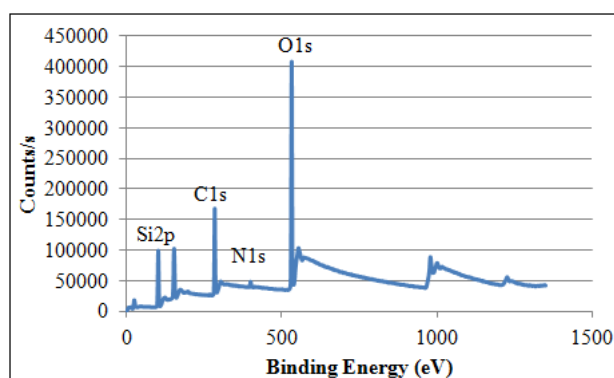


**Figure 4.18** XPS survey spectrum of Trp-SAM (10mM, 2h) modified PDMS substrate.

XPS analysis for Si2p, C1s, O1s and Ni1s core levels of Trp-SAM (10mM, 2h) modified PDMS substrates were measured by using Thermo Scientific K-Alpha XPS and shown in the Figure 4.19. As seen from the figure, Si-C and Si-O bonds were

found in Si2p region at 102,1 and 103,8 eV [42]. In C1s core level; peaks were found at 286.2, 284.6, 285.2 and 288,6 eV corresponding to C-Si, C-C, C=O and C-N bonds [42, 43, 44, 46]. In O1s level, Si-O, C=O bonds was shown at 532,6 and 533,3 eV, and in N1s level, C-N bond was found at 400,0 eV [42, 46, 45].

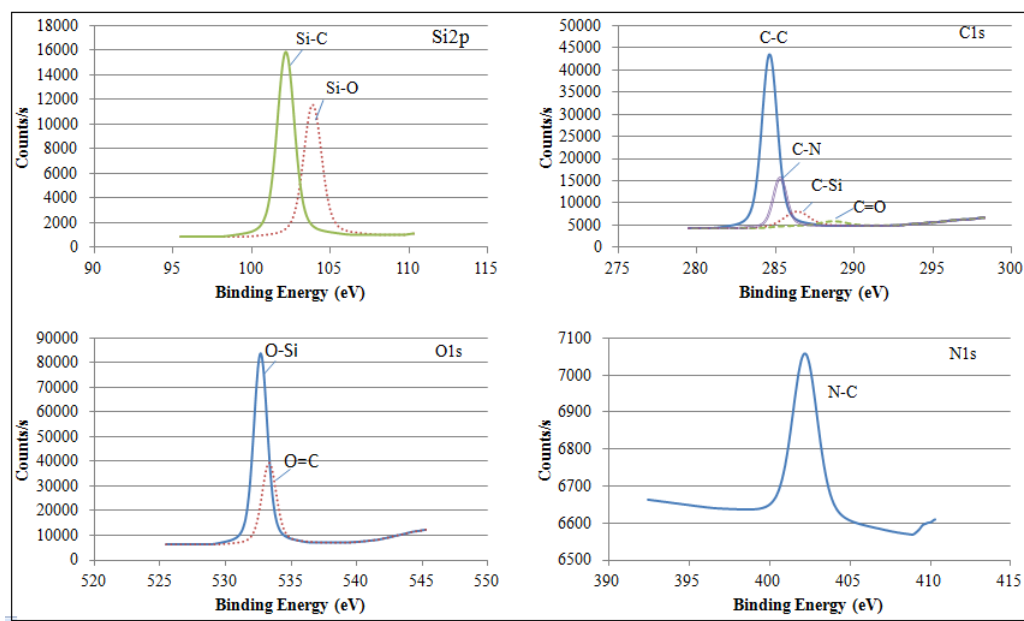


**Figure 4.19** XPS spectra of Trp-SAM (10mM) modified PDMS with Si2p, C1s, O1s and N1s regions.

Atomic percentages of the Trp-SAM modified PDMS components (C, O, N, Si) were calculated from the area under the curves, as 34.86, 35.06, 1.94 and 28.14% for C, O, N and Si atoms, respectively. Comparison of measured atomic percentages with theoretical ones were shown in the Table 4.11

**Table 4.11**

Theoretical and measured atomic percentages of C, O, N and Si atoms found in Trp-SAM modified PDMS.

	Theoretical Atomic %	Measured Atomic %
C	56.67	34.86
O	20.00	35.06
N	10.00	1.94
Si	13.33	28.14

#### 4.5.6 XPS analysis of Type II Collagen Modified PDMS Substrates

XPS analysis of Type II collagen (0,1mg/mL, 24h, at 4°C) modified PDMS substrates prepolymer/crosslinker ratio of 10:1 (w/w) were done by using Thermo Scientific K-Alpha XPS. XPS survey spectrum of Type II collagen (0,1mg/mL, 24h, at 4°C) modified PDMS substrates were shown in the Figure 4.20. According to the figure, Si2p, C1s, N1s and O1s peaks were found from the analysis.

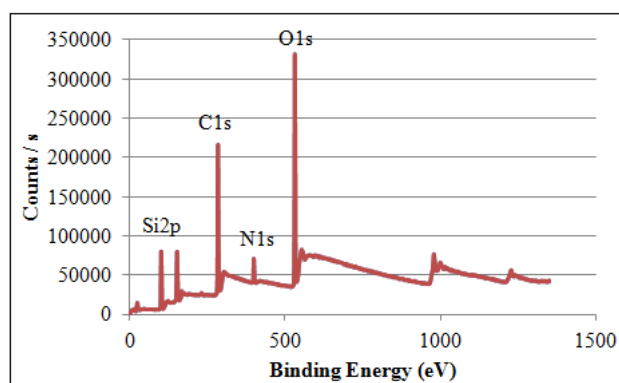


**Figure 4.20** XPS survey spectrum of Type II collagen modified PDMS substrate.

XPS analysis for Si2p, C1s, O1s and N1s core levels of Type II collagen modified PDMS substrates were measured by using Thermo Scientific K-Alpha XPS and shown in the Figure 4.21. As seen from the figure, Si-C and Si-O bonds were found in Si2p region at 101.9 and 103.3 eV [42]. In C1s core level; peaks were found at 285.9, 284.6, 285.2 and 288.1 eV corresponding to C-Si, C-C, C=O and C-N bonds [42, 43, 44, 46]. In O1s level, Si-O, C=O and C-O bonds was shown at 532.2, 532.9 and 531.4 and in N1s level, C-N bond was found at 400.0 eV [42, 46, 45].

Atomic percentages of the Type II collagen modified PDMS components (C, O, N, Si) were calculated from the area under the curves, as 49.10, 25.90, 4.08 and 20.88% for C, O, N and Si atoms, respectively.

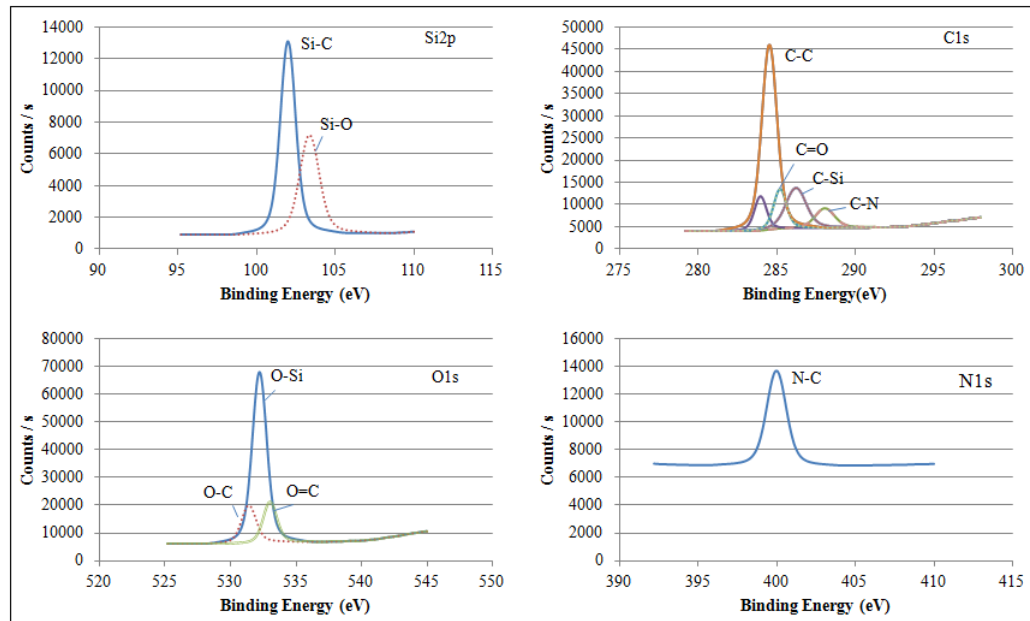


**Figure 4.21** XPS spectra of Type II collagen modified PDMS with Si2p, C1s, O1s and N1s regions.

**Table 4.12**

Theoretical and measured atomic percentages of C, O, N and Si atoms found in Type II collagen modified PDMS.

Atom	Measured Atomic %
C	25.90
O	49.14
N	20.88
Si	4.08

## 5. DISCUSSION

Recent studies have shown the effects of preparing mimicked structures on cell behaviour (adhesion, cell growth, migration, proliferation) and stem cell differentiation [9, 47, 48, 30]. With the inspiration of these studies cartilage mimicked structures were prepared in this thesis. The main objectives of the thesis could be identified as

- The production of polydimethylsiloxane (PDMS) cell substrates mimicking cartilage tissue's elasticity,
- Adjusting the surface topography of substrates to the type II collagen fibers, which are found predominantly (approximately 90% of total collagen) [2] in cartilage tissue,
- Modifying the surface with amino acid conjugated self assembled molecules and to characterize these substrates,
- Modifying the surface with type II collagen and to characterize these substrates.

### 5.1 Stiffness of PDMS substrates

In this thesis, PDMS was used as a possible cell substrate as it is a widely used inert, biocompatible and nontoxic polymer with tunable mechanical properties.[49] In order to prepare substrates with cartilage tissue's stiffness (0.45 to 0.80 MPa) [13], PDMS substrates were produced with different prepolymer/crosslinker ratios (10:1, 15:1, 20:1 and 30:1). Young's moduli of these PDMS substrates with different prepolymer/crosslinker ratios were measured with nanoindenter (CellHesion<sup>®</sup>, JPK, Germany). Nanoindentation data were recorded on the system and Hertz model was applied on this data by using the software of the system. Young's moduli range of PDMS substrates with different prepolymer-crosslinker ratios, 10:1, 15:1, 20:1 and 30:1, were

found to be  $2.13 \pm 0.16$  MPa,  $1.47 \pm 0.07$  MPa,  $0.72 \pm 0.05$  MPa and  $0.56 \pm 0.06$  kPa, respectively. Thus, PDMS substrates with prepolymer/crosslinker ratios of 20:1 and 30:1 were fit the range of healthy cartilage's stiffness (0.45 to 0.80 MPa) [49, 13]. According to these measurements, concentration of crosslinker was directly proportional to the stiffness (Young's modulus) of the PDMS. Also the difference between Young's moduli values were getting lower with decreasing amount of crosslinker as the difference between 10:1 and 20:1 is much higher than 20:1 and 30:1.

## 5.2 Surface Topography of PDMS Substrates

There are several ongoing studies on mimicked topography on cell substrates as it improves the biocompatibility of substrates, regulates cell adhesion, spreading and migration [50, 51]. In local micro-environment of cells, they collect physical and chemical signals and change their behavior according to this data. For example, there is a specific interaction between cell surface receptors and extracellular matrix. Nanotopographies were proved to stimulate adsorption of ECM proteins [52]. In cartilage tissue, type II collagen is the predominant collagen and provides compressive load strength to the cartilage tissue by forming a meshwork. Thus its function is crucial for cartilage tissue. Near the joint surface (superficial zone of cartilage) type II collagen orientation is parallel. In this thesis, this parallel alignment of type II collagen was mimicked with varying dimensions [size of line width was changed to be 100, 150, and 200  $\mu\text{m}$  (A), size of line length was changed to be 30, 40 and 50  $\mu\text{m}$  (B), while the perpendicular period was changed to be 30, 40 and 50  $\mu\text{m}$  (C)]. A template was designed according to these dimensions and PDMS surfaces were patterned by using soft lithography. Patterned surface topographies on PDMS substrates were analyzed with optical microscopy and it was shown that patterns were mimicked properly.

### 5.3 Chemical modifications of PDMS substrates

PDMS is a highly hydrophobic polymer and has no cell binding sites. Therefore, surface modifications are essential for PDMS as a cell substrate [52]. Effects of chemical modification of cell substrates on cell adhesion, protein absorption, proliferation and stem cell differentiation were proved, but novel strategies are still required to enhance better cell-substrate interactions [10, 49].

In this thesis chemical and biochemical alterations were done on PDMS substrates with different prepolymer/crosslinker ratios (10:1, 15:1, 20:1 and 30:1). As discussed before, prepolymer/crosslinker ratio determines PDMS's stiffness. According to contact angle results, this ratio also effects surface wettability of PDMS substrates. This means the surface chemistry of substrates with different crosslinker concentrations were not similar. With decreasing crosslinker concentrations, there was an increase found in the amount of uncrosslinked hydroxyl groups in PDMS [49]. However, this situation was important only for cell culture experiments investigating the effects of only stiffness, without any chemical modifications of surface. Since in this thesis, for all surface modifications, substrate surface was hydroxylated by using oxygen plasma treatment which could eliminate effects of crosslinker concentration. That was why, surface characterization of PDMS substrates were only performed for PDMS with a prepolymer-crosslinker ratio of 10:1.

Modifications of surface chemistry alters the hydrophobicity of the substrates and consequently influences protein absorption capabilities of these materials [10]. PDMS has methyl (-CH<sub>3</sub>) groups which makes it a relatively hydrophobic polymer. It is known from the literature that amino (-NH<sub>2</sub>) groups were more hydrophilic and modification with molecules including amino (-NH<sub>2</sub>) groups has proved effects on the enhancement of cell-substrate interactions [10]. In this thesis amino acid conjugated self-assembled molecules (His-SAM, Leu-SAM and Trp-SAM) were used for the modification of cell substrates contained. Since they include amino (-NH<sub>2</sub>), increased cell-substrate interactions were expected from the beginning. Besides including amino (-NH<sub>2</sub>) groups, they were amino acids, the monomers of proteins, since modification with these molecules made our substrates not only more suitable for protein absorption, but also provided more extracellular matrix-like biochemistry.



In this thesis, using SAMs for chemical alterations enabled us to modify substrates in an easier and more stable way. Three different amino acid conjugated self-assembled molecules; His-SAM, Leu-SAM and Trp-SAM were synthesized to modify PDMS substrates. For the characterization of amino acid conjugated SAMs which were known as Cbz-AA-Bt,  $^1\text{H}$  NMR was used. In  $^1\text{H}$  NMR spectra of Cbz-AA-Bt compounds, doublet signals were obtained at 8.15 and 8.30 ppm and triplet signals were obtained around 7.50-7.20 ppm which were characteristic signals of N-substitute benzotriazole. Thus, binding of benzotriazole to Cbz-AA-Bt was proved. Also the 5 protons of aromatic signals at 7 ppm and 2 protons of aliphatic singlet signals were supported the existence of Cbz group. In later steps, by-products (Abz-AA-amines) were obtained from nucleophilic substitution reactions. Existence of this products were proved from the disappearance of N-substitute benzotriazole's specific signals and recognition of aliphatic  $\text{CH}_2$  signals of amine group (3.0, 1.5 ppm and 0.6 ppm) which was bound to Si. In the last step, Cbz group was pulled off by using catalytic hydrogenation and free amine function was obtained. Aromatic phenyl ring at 7ppm and disappearance of  $-\text{CH}_2$  signals (at 3-4ppm) were proved this reaction.

APTES molecule was existed in all of the amino acid conjugated self assembled molecules besides its role in type II collagen modification. Therefore, to investigate the success of chemical modifications of cell substrates, contact angle measurements and XPS analysis were done and compared with APTES modified and bare PDMS substrates. Before any modification, contact angle results of PDMS were relatively high ( $104.1^\circ \pm 5.1$ ). Then, to activate PDMS surfaces, plasma oxygen treatment was done resulting the formation of hydroxyl groups on the surface. Hydroxyl groups make PDMS highly hydrophilic and also ready for any reactions [39]. After APTES modification, contact angle measurements of substrates were found to be  $61.98^\circ \pm 5.5$  which proved APTES was bound to the surface and its contact angle was also similar to literature [38].

In order to find the optimum concentration and dipping time for the amino acid conjugated SAMs, PDMS substrates were modified with a range of His-SAM concentrations (1-20mM, 2h) and dipping time (1h-24h). For both of them, it was shown that, contact angle values were a function of concentration and dipping time. According to contact angle measurements, His-SAM modified PDMS substrates were become less

hydrophobic (around  $90^\circ$ ) than bare PDMS ( $104.1^\circ$ ) which proved the success of modification and also made substrates more suitable for cell interactions. Contact angle values of His-SAM modified substrates were decreased in the increasing concentrations of 1 mM to 20 mM, except 10 mM. This decrease was caused from the functional imidazole and carboxylic acid groups or the minority of the covered area of the surface. In the modifications of substrates with 10 mM His-SAM, contact angle value was increased slightly which was resulted from the orientation of the molecules with a specific angle and the repulsion between imidazole and carboxylic acid groups (polar groups). As a consequence, hydrophobic alkyl groups of APTES were become apparent and increased the hydrophobicity of the substrate.

Contact angle values showing the effect of His-SAM dipping time were increased with time except for 4h. The increase in the angles with dipping time was caused from the orientation of the molecule as discussed before.

To achieve more reliable results, XPS (XPS, Thermo Scientific K- $\alpha$ , Germany) analysis of bare, APTES, His-SAM, Leu-SAM, Trp-SAM and type II collagen modified substrates were performed with Al K $\alpha$  X-radiation. From the obtained XPS spectra, characteristic Si2p, C1s, N1s and O1s signals' areas were investigated and with these values, atomic percentages were calculated. Only for bare PDMS, there was no N1s signal, as there are no N atoms in this polymer. In all other modifications, N1s signals were shown, proving the success of surface alterations. In the XPS data of APTES modified PDMS, all specific bonds were shown, as Si-O, Si-C, C-C and C-N. However, theoretical and measured atomic percentages were not exactly the same. As the specific atom was N in APTES modified PDMS with regard to bare PDMS, determination of surface coverage could be done according to the amount of N. From these values (theoretical 5.9% whereas measured to be 1.65%), it could be said that 28% of the surface was covered with APTES which was a quite proper percentage as one APTES molecule requires three hydroxyl (-OH) groups to bind on PDMS surface and this situation blocks full coverage for all molecules (His-SAM, Leu-SAM, Trp-SAM and type II collagen) binding on PDMS with APTES side.

From the area under the XPS spectra of PDMS substrates modified with different concentrations of His-SAM (1-20 mM, 2 h), maximum atomic percentage of N was calculated to be 3.41% for 10 mM His-SAM, as it was 14.81% theoretically. This

means, maximum coverage of His-SAM was achieved with 10 mM of His-SAM. For the dipping time investigation, hydroxylated PDMS substrates were dipped in 10 mM His-SAM solution for 1h-24h. The maximum coverage (max N atomic percentage) was calculated for the dipping time of 24h which was 4.69%. However for timesaving reason, the optimum concentration was selected to be 2h in which N concentration was 3.41%.

Surface modifications of substrates with Leu-SAM and Trp-SAM, concentration and dipping time were fixed to 10mM and 2h after optimization by using His-SAM. In the XPS analysis of Leu-SAM (10 mM, 2h) modified PDMS substrates, in Si2p, C1s, O1s and N1s core levels, all specific Si-C and Si-O bonds (101.9 and 103.0 eV), C-Si, C-C, C=O and C-N bonds (285.2, 284.4, 286.3 and 288.2 eV) and Si-O, C=O bonds (532.1 and 532.9 eV) and C-N (400.0 eV) bonds were found which means the surface modification was proved [41, 42, 43, 44, 46, 45]. Also atomic percentage of N was calculated to be 3.36% as it was 8.33% theoretically. Thus, 40% of the substrate surface was covered with Leu-SAM.

For the XPS characterization of Trp-SAM modified substrates, all specific bonds of the molecule were found from their specific binding energies as Si-C and Si-O (102,1 and 103,8 eV.), to C-Si, C-C, C=O and C-N (286.2, 284.6, 285.2 and 288,6 eV.), Si-O, C=O (532.6 and 533.3 eV) and C-N bond (400.0 eV) [42, 43, 44, 46, 45, 49]. Surface coverage of Trp-SAM was approximately 20%. This coverage percentage was quite proper, as tail groups of Trp-SAM are larger and when they are close to each other there would be repulsive forces between their indole groups. Also, Trp-SAM was bound to PDMS substrate from its APTES side. As discussed before, one APTES molecule requires three  $\text{OH}$  groups to bind on PDMS surface and this situation decreases the percentage of coverage.

Type II collagen is found predominantly (approximately 90% of total collagen) in the extracellular matrix of cartilage [1]. Thus modification of substrate with type II collagen enables a more extracellular matrix-like environment for cell cultures. Collagen is a protein composed of many amino acids and consequently it includes many atoms. The most common tripeptide in collagen is composed of glycine (Gly), proline (Pro) and hydroxyproline (Hyp)[48]. This tripeptide includes C, O, N and H. To show the collagen type II modification, XPS analysis was done and from its spectrum, Si2p

(from PDMS), C1s, O1s and N1s peaks were obtained. Also as seen from Figure 4.21, all specific binds of Collagen type II were shown on the XPS spectra as C-C, C=O and C-N.

In conclusion, characterization results showed that, stiffness adjustments, surface chemistry and surface topography were obtained successfully and these modified substrates with cartilage like stiffness, chemistry and topography are possible cell substrates for cartilage tissue engineering.

## 5.4 Future Work

The idea of preparing cell substrates with cartilage like stiffness, chemistry and topography was supported with the characterization results of this study. Thus, investigation of the interactions between these modified cell substrates and primary chondrocytes or stem cells would be a promising work for cartilage tissue engineering.

## REFERENCES

1. Oatis, C. A., *Kinesiology: The Mechanics and Pathomechanics of Human Movement*, Lippincott Williams and Wilkins, 2008.
2. Jiang, J., S. B. Nicoll, and H. H. Lu, "Co-culture of osteoblasts and chondrocytes modulates cellular differentiation in vitro," *Biochem Biophys Res Commun.*, Vol. 16, pp. 762–770, 2005.
3. Chian, H., and J. J. Jiang, "Repair of articular cartilage defects: Review and perspectives," *J Formos Med Assoc.*, Vol. 108, pp. 81–101, 2009.
4. Steinwachs, M. R., T. Guggi, and P. C. Kreuz, "Marrow stimulation techniques," *Injury*, Vol. 39, pp. 26–31, 2008.
5. Rohde, R. S., R. K. Stude, and C. R. Chu, "Mini-pig fresh osteochondral allografts deteriorate after 1 week of cold storage," *Clin Orthop Relat Res.*, Vol. 427, pp. 226–233, 2004.
6. Jackson, D. W., M. J. Scheer, and T. M. Simon, "Cartilage substitutes: Overview of basic science and treatment options," *J Am Acad Orthop Surg*, Vol. 9, pp. 37–52, 2001.
7. Sharma, S. G., A. K. Dinda, and N. C. M., "Cartilage tissue engineering: current scenario and challenges," *RSV Adv.*, Vol. 2, pp. 90–99, 2011.
8. Rosenzweig, D. H., S. S. Cafaggi, and T. M. Quinn, "Functionalization of dynamic culture surfaces with a cartilage extracellular matrix extract enhances chondrocyte phenotype against dedifferentiation," *Acta Biomaterialia*, Vol. 8, pp. 3333–3341, 2012.
9. Engler, F. A. R. J., A. Eckhardt, F. Ahmed, and D. E. Discher, "Cell responses to the mechanochemical microenvironment, implications for regenerative medicine and drug delivery," *Advanced Drug Delivery Reviews*, Vol. 59, pp. 1329–1339, 2007.
10. X Liua, X., Q. Feng, A. Bachhukab, and K. Vasilev, "Surface chemical functionalities affect the behavior of human adipose-derived stem cells in vitro," *Applied Surface Science*, Vol. 270, pp. 473–479, 2013.
11. Cigognini, D., A. Lomas, P. Kumar, A. Satyam, A. English, A. Azeem, A. Pandit, and D. Zeugolis, "Engineering in vitro microenvironments for cell based therapies and drug discovery," *Drug Discovery Today*, Vol. 13, pp. 1099–1108, 2013.
12. Eberli, D., *Tissue Engineering for Tissue and Organ Regeneration*, Intech, 2011.
13. Mahmoudifar, N., and P. M. Doran, "Chondrogenesis and cartilage tissue engineering: the longer road to technology development," *Trends in Biotechnology*, Vol. 30, pp. 166–176, 2012.
14. Tumer, C. H., S. C. Cowin, J. Y. Rho, R. B. Ashman, and J. C. Rice, "The fabric dependence of the orthotropic elastic constants of cancellous bone," *J. Biomech.*, Vol. 22, pp. 549–561, 1990.
15. Huey, D. J., J. C. Hu, Kyriacos, and A. Athanasiou, "Bone, cartilage regeneration remains elusive," *Science*, Vol. 338, pp. 917–921, 2012.
16. Setton, L., "Polymer therapeutics: Reservoir drugs," *Nature Materials*, Vol. 7, pp. 172–174, 2008.

17. David, E., "Collagen of articular cartilage," *Arthritis Res*, Vol. 4, pp. 30–35, 2002.
18. Johnson, D., *Practical Orthopaedic Sports Medicine and Arthroscopy*, Lippincott Williams and Wilkins, 2007.
19. Klein, J., "Repair or replacementâa joint perspective," *Science*, Vol. 323, pp. 47–48, 2009.
20. Kessler, M. W., G. Ackerman, J. S. Dines, and D. Grande, "Emerging technologies and fourth generation issues in cartilage repair," *Sports Med Arthrosc*, Vol. 16, pp. 246–254, 2008.
21. Steinwachs, M., and P. C. Kreuz, "Autologous chondrocyte implantation in chondral defects of the knee with a type i/iii collagen membrane: a prospective study with a 3-year follow-up," *Arthroscopy*, Vol. 23, pp. 381–387, 2007.
22. Can, A., and S. Karahuseyinoglu, "Concise review: human umbilical cord stroma with regard to the source of fetus-derived stem cells," *Stem Cells*, Vol. 25, pp. 2886–2895, 2007.
23. Weiss, M. L., K. E. Mitchell, J. E. Hix, S. Medicetty, S. Z. El-Zarkouny, D. Grieger, and D. L. Troyer, "Transplantation of porcine umbilical cord matrix cells into the rat brain," *Exp. Neurol.*, no. 182, pp. 28–29, 2003.
24. Weiss, M. L., S. Medicetty, A. R. Bledsoe, R. S. Rachakatla, M. Choi, S. Merchav, Y. Luo, M. S. Rao, G. Velagaleti, and D. Troyer, "Human umbilical cord matrix stem cells: preliminary characterization and effect of transplantation in a rodent model of parkinsonâs disease," *Stem Cells*, Vol. 24, pp. 781–792, 2006.
25. Li, Y., H. W. Cheng, K. M. C. Cheung, D. Chan, and B. P. Chan, "Mesenchymal stem cell-collagen microspheres for articular cartilage repair: Cell density and differentiation status," *Acta Biomaterialia*, 2014. in press.
26. Kobel, S. A., and M. P. Lutolf, "Materials as artificial stem cell microenvironments," *Comprehensive Biomaterials*, Vol. 2, pp. 155–167, 2011.
27. Engler, A., S. Sen, H. L. Sweeney, and D. E. Matrix, "Elasticity directs stem cell lineage specification," *Cell*, Vol. 126, pp. 677–689, 2006.
28. Guliak, F., "Control of stem cell fate by physical interactions with the extracellular matrix," *Cell Stem Cell*, Vol. 5, pp. 17–26, 2009.
29. Ahn, E. H., Y. Kim, S. S. A. Kshitiz, J. Afzal, S. Lee, M. Kwak, K. Y. Suh, D. H. Kim, and A. Levchenko, "Spatial control of adult stem cell fate using nanotopographic cues," *Biomaterials*, Vol. 35, pp. 2401–2410, 2014.
30. Stein, G. S., and J. B. Lian, "Molecular mechanisms mediating proliferation and differentiation interrelationships during progressive development of the osteoblast phenotype," *Endocrine Review*, Vol. 14, pp. 424–442, 1993.
31. Dular-Tulloch, A. J., R. Bizios, and R. W. Siegel, "Differentiation of human mesenchymal stem cells on nano- and micro-grain size titania," *Materials Science and Engineering*, Vol. 31, pp. 357–362, 1993.
32. Chiellini, F., A. M. Piras, and E. Chiellini, "Polymeric materials for bone and cartilage repair," *Progress in Polymer Science*, Vol. 35, pp. 403–440, 2010.

33. Bartalena, G. Y., T. Loosli, T. Zambellid, and J. G. Snedeker, "Biomaterial surface modifications can dominate cell-substrate mechanics: the impact of pdms plasma treatment on a quantitative assay of cell stiffness," *Soft Matter*, Vol. 8, pp. 673–681, 2012.
34. Casettari, L., D. Vllasaliu, J. K. W. Lam, M. Soliman, and L. Illum, "Biomedical applications of amino acid-modified chitosans: A review," *Biomaterials*, Vol. 33, pp. 7565–7583, 2013.
35. Arnold, M., "Activation of integrin function by nanopatterned adhesive interfaces," *Chemphyschem*, Vol. 5, pp. 383–388, 2004.
36. Fredonnet, J., J. Foncy, S. Lamarre, J. C. Cau, E. Trevisiol, J. P. Peyrade, J. M. Francois, and C. Severac, "Dynamic pdms inking for dna patterning by soft lithography," *Microelectronic Eng*, Vol. 111, pp. 379–383, 2013.
37. Wipff, P. J., H. Majda, C. Acharya, L. Buscemi, J. J. Meister, and B. Hinz, "The covalent attachment of adhesion molecules to silicone membranes for cell stretching applications," *Biomaterials*, Vol. 30, pp. 1781–1789, 2009.
38. Lee, N. Y., and B. H. Chung, "Novel poly(dimethylsiloxane) bonding strategy via room temperature chemical gluing," *Langmuir*, Vol. 25, pp. 3861–3866, 2009.
39. Hong, Y., C. Gao, Y. Xie, Y. Gong, and J. Shen, "Collagen-coated polylactide microspheres as chondrocyte microcarriers," *Biomaterials*, Vol. 26, pp. 6305–6313, 2005.
40. JPKInstruments, "Cellhesion user manual software release 4.2," pp. 128–130, 2012.
41. Briggs, D., and M. P. Seah, "Practical surface analysis," *Surface and Interface Analysis*, Vol. 20, pp. 1081–1082, 1993.
42. Angelis, B. A., C. Rizzo, S. Contarini, and S. P. Howlett, "Xps study on the dispersion of carbone additives in silicon carbide powders," *Applied Surface Science*, Vol. 51, pp. 177–183, 1991.
43. Moncoffre, N., G. Hollinger, H. Jaffrezic, G. Marest, and J. Tousset, "Xps study on the dispersion of carbone additives in silicon carbide powders," *Applied Surface Science*, Vol. 51, pp. 177–183, 1991.
44. Unger, W. E. S., T. Gross, O. Bose, A. Lippitz, T. Fritz, and U. Gelius, "Evaluation of static charge stabilization and determination methods in xps on non-conducting samples," *Surface and Interface Analysis*, Vol. 29, pp. 535–543, 2000.
45. Bagreev, A., G. Nanse, J. Lahay, and V. Strelko, "Porous structure and surface chemistry of nitrogen containing carbons from polymers," *Carbon*, Vol. 37, pp. 585–590, 1999.
46. Bismarck, A., R. Tahhan, J. Springer, A. Schulz, T. M. Klapijtk, H. Zell, and W. Michaeli, "Influence of fluorination on the properties of carbon fibres," *Journal of Fluorine Chemistry*, Vol. 84, pp. 127–134, 1997.
47. Curran, J. M., R. Chen, and J. A. Hunt, "The guidance of human mesenchymal stem cell differentiation in vitro by controlled modifications to the cell substrate," *Biomaterials*, Vol. 27, pp. 4783–4793, 2006.
48. Puppi, D., F. Chiellini, A. M. Piras, and E. Chiellini, "Polymeric materials for bone and cartilage repair," *Progress in Polymer Science*, Vol. 35, pp. 403–440, 2010.

49. Brown, X. Q., K. Ookawa, and J. Y. Wong, "Evaluation of polydimethylsiloxane scaffolds with physiologically relevant elastic moduli: interplay of substrate mechanics and surface chemistry effects on vascular smooth muscle cell response," *Biomaterials*, Vol. 26, pp. 3123–3129, 2005.
50. Kim, P., D. H. Kim, B. Kim, S. K. Choi, S. H. Lee, A. Khademhosseini, R. Langer, and K. Y. Suh, "Fabrication of nanostructures of polyethylene glycol for applications to protein adsorption and cell adhesion," *Nanotechnology*, Vol. 16, no. 10, pp. 2420–2430, 2005.
51. Yima, E. K. F., E. M. Darlinga, K. Kulangara, F. Guilaka, and K. W. Leong, "Nanotopography-induced changes in focal adhesions, cytoskeletal organization, and mechanical properties of human mesenchymal stem cells," *Biomaterials*, Vol. 31, pp. 1299–1306, 2010.
52. Lee, J. N., C. Park, and G. M. Whitesides, "Solvent compatibility of pdms based microfluidic devices," *Analytical Chemistry*, Vol. 75, pp. 6544–6554, 2003.